THESIS

THE DISCOVERY OF NOVEL PROTEINS REGULATING MELANOSOME BIOGENESIS AND FUNCTION

Submitted by

Anna Detry

Department of Biochemistry and Molecular Biology

In partial fulfillment of the requirements

For the Degree of Master of Science

Colorado State University

Fort Collins, Colorado

Spring 2022

Master's Committee:

Advisor: Santiago Di Pietro

Jeffrey Hansen
Frederic Hoerndli

ABSTRACT

THE DISCOVERY OF NOVEL PROTEINS REGULATING MELANOSOME BIOGENESIS AND FUNCTION

Melanosomes are lysosomal related organelles found in cells which are responsible for making pigment such as skin melanocytes. They are membrane bound organelles that form from the endosomal pathway and have specific proteins and enzymes which allow them to perform the function of melanin production. The process of melanosome biogenesis involves the melanosomes developing through four stages that are classified by electron microscopy appearance. The different melanosome stages have amyloid fibrils formed by proteolytically processed PMEL protein, different amounts of melanin, and different melanosomal proteins. In addition to melanosome biogenesis, another key factor in proper melanin formation and pigmentation is the melanosome luminal pH. The melanin producing enzyme tyrosinase is a pH dependent enzyme. When melanosomes are more acidic, tyrosinase is less functional, leading to less melanin production and a hypopigmentation phenotype. The Di Pietro lab and others have shown that the Two Pore Channel Two (TPC2) is a key regulator of melanosome pH, as well as a regulator of melanosome size and localizes to melanosome membranes. A proximity-dependent biotin identification experiment was preformed using TPC2 and eight potential melanosome proteins were identified. Each of these candidate proteins were knocked down in a human melanoma cell line using small interfering RNA and studied for a potential pigmentation phenotype. Tetraspanin10, phospholipase D1, myosin heavy chain 9, and myosin heavy chain 10 all showed a hypopigmentation phenotype. Two independent tetraspanin 10 knockout cell lines

were generated using CRISPR-Cas9 which reproduced the hypopigmentation phenotype. In addition, the phenotype was rescued by re-expressing tetraspanin 10 in the knockout cells and overexpressing tetraspanin 10 in wild type cells showed a hyperpigmentation phenotype. This shows that tetraspanin 10 is involved in the pigmentation process. CD63 is another tetraspanin known to play vital roles in melanosome biogenesis and based on the minimal information aviable on tetraspanin 10, it can be hypothesized as being involved in PMEL processing. The discovery that tetraspanin 10 is involved in skin pigmentation will lead to better understanding of the pigmentation process and pigmentation related diseases.

ACKNOWLEDGMENTS

I would like to thank Santiago Di Pietro, Wyatt Beyers, and the rest of the Di Pietro lab for all their assistance and support throughout my time in the lab. I would also like to thank my master's committee for their guidance on this project and O'Neil Wiggan for providing siRNA for MYH9 and MYH10. My family and friends have been my biggest supporters and deserve much thanks too. In addition, I would like to thank the NIH for the funding that made this project possible.

TABLE OF CONTENTS

CHAPTER 1: INTRODUCTION

What are melanosomes?

Specific cells within the human body perform specialized functions and are directly related to certain aspects of a living organism. Pigmentation of skin, hair, and eyes comes from melanin, which is produced by specialized cells and organelles. In humans, skin pigmentation is formed by melanin producing cells called epithelial melanocytes[1]. Melanocytes have long cellular extensions which interact with surrounding keratinocytes. Eye pigmentation is formed by melanin producing cells called retinal pigment epithelial cells[2]. Within melanocytes and retinal pigment cells are specialized membrane bound organelles called melanosomes.

Melanosomes are large membrane bound organelles responsible for generation and distribution of melanin[1,3]. Melanosomes are lysosome related organelles and develop through four stages. Stage one melanosomes are undifferentiated vesicles that lack pigmentation. They undergo a complex biogenesis process to form heavily pigmented stage four melanosomes. These stage four melanosomes within epithelial melanocytes are transported through unknown mechanisms to neighboring cells, keratinocytes[1]. Melanosomes protect from UV-induced DNA damage and are responsible for skin pigmentation. Retinal pigment epithelial cells do not release the fully developed melanosomes like epithelial melanocytes do. These cells keep the melanosomes and are directly responsible for eye pigmentation and absorbing scattered light[1]. Defects in melanosome biogenesis often result in oculocutaneous albinism with increased skin damage and poor visual activity.

The large size of melanosomes makes them an ideal organelle to study biogenesis and differentiation processes; however, much remains unknown about melanosomes. 125 genes

directly related to melanosomes and pigmentation have been identified of which several of the corresponding proteins still have unknown roles[3]. Some of these proteins are known to be specific to melanosomes, and others are found in many lysosome-related organelles and granules. Even with all the unanswered questions and lack of finer details about melanosomes, it is well understood that they are the foundation of proper pigmentation and are necessary for melanin production.

Overview of melanosome biogenesis

The synthesis of an organelle is a complex process and melanosome biogenesis is no exception. Melanosome biogenesis involves many proteins and cell signals to properly traffic enzymes and form a melanosome. While much of the mechanism has been characterized, parts of the process remain unknown. Melanosomes are lysosome-related organelles which develop from early endosomes and form through a four-stage process[1]. These stages are classified by the appearance of the melanosome in electron microscopy images.

Within the endosomal network protein complexes BLOC-1, BLOC-2, AP-1, and AP-3 sort proteins and ensure that the necessary proteins are transported to the forming melanosomes[1]. Stage one melanosomes form from the early endosome. These melanosomes contain the protein PMEL on their limiting membrane. During stage one, the limiting membrane invaginates and pinches off forming small (approximately 50nm) vesicles in the lumen of the organelle that contains the PMEL protein. This PMEL gets processed, cleaved, and forms a functional amyloid matrix which is governed by o-glycans[4]. Once the melanosome has PMEL striations, it is a stage two melanosome. Other melanosome proteins, including tyrosinase (Tyr), tyrosinase related proteins 1 and 2 (TYRP1 and TYRP2), are transported to the forming melanosome on vesicles which also contain Rab32 and Rab38. Tyrosinase and tyrosinase related proteins are integral

membrane proteins with their catalytic sites exposed to the lumen of the organelle. Once they arrive at the stage two melanosome, they begin synthesis of melanin, and the melanin settles on the PMEL striations, making a stage three melanosome[1]. Next, the melanin begins to accumulate on the PMEL striations, and the melanosome becomes full of melanin[5]. This is now considered a stage four, fully developed melanosome.

Fully developed melanosomes are then transported to keratinocytes through mechanisms which are still being studied. Melanosomes are moved throughout the melanocyte on microtubules then captured by myosin and actin at the melanocyte dendrite tip[6]. After being transported to the dendrite tip the melanin is transferred from the melanocyte to the keratinocyte in ways which are still being characterized. Most evidence suggests the melanosome membrane fuses with the melanocyte plasma membrane[7]. Other evidence supports the dendrite tip breaks off creating a vesicle containing melanosomes which is endocytosed by the keratinocyte or that the melanocyte plasma membrane fuses with the keratinocyte plasma membrane transferring melanosomes from one cell to the other[7]. While melanosome biogenesis is one of the most common vesicle transport mechanisms studied, the specific roles of many proteins involved in this biogenesis process remain unknown while others are well studied and characterized.

TPC2 Biotin Identification Experiment

Another key factor in proper melanin formation and pigmentation, is the melanosome luminal pH. Na^+/H^+ antiporters, V-ATPases, and Oculocutaneous Albinism 2 (OCA2), a major melanosome chloride channel, regulate melanosome pH[8,9]. Melanin producing enzyme, tyrosinase, is a pH dependent enzyme. When melanosomes are more acidic, tyrosinase is less functional, leading to less melanin production and a lighter pigmentation phenotype[10]. It has been shown that the Two Pore Channel Two (TPC2) is another regulator of melanosome pH, as

well as a regulator of melanosome size and localizes to melanosome membranes[11,12]. TPC2 knockout cells have been shown to have increased pigmentation, a less acidic melanosome lumen, larger melanosomes and have increased levels of tyrosinase[11,13]. Polymorphisms of TPC2, M484L and G734E, have been associated with the shift from brown to blonde hair in Europeans[14]. While there is strong evidence that TPC2 is a key protein in melanosome regulation and pigmentation, the mechanism by which TPC2 functions in melanosomes and pigmentation is still unclear. To address this gap in knowledge, Wyatt Beyers performed a proximity-dependent biotin identification[15] (BioID) experiment by expressing the promiscuous biotin ligase BioID2 fused to TPC2 with the goal of identifying proteins in the proximity of TPC2. From this experiment the Di Pietro lab developed a list of eight potential melanosome proteins not previously known to function at melanosomes (Table 1). Based on these proteins potentially being in the proximity of TPC2, we hypothesized that they may also be pigmentation related proteins and aim to determine their involvement in pigmentation. One of these proteins, OCA7, has been well studied in our lab throughout the past few years and demonstrated to be localized to melanosomes and to regulate melanosome function. This result provides confidence the screening has uncovered new proteins involved in melanosome function. However, the other seven proteins have yet to be characterized.

The investigation into the candidate proteins involvement in pigmentation will help develop a full understanding of melanosome biogenesis and pigmentation. Mutations in many of the known proteins in melanosome biogenesis have been linked to pigmentation diseases. For example, mutations in tyrosinase, tyrosinase related proteins 1 and 2, and OCA2 lead to oculocutaneous albinisms, and mutations in BLOC-2 are associated with Hermansky-Pudlak syndrome which presents with oculocutaneous albinism and other manifestations[16,17]. While

there are many known pigmentation diseases, the mechanism behind them is often unknown making treatments difficult. By discovering novel melanosome proteins, a better understanding of the overall pigmentation process can be obtained. This can potentially lead to a greater understanding of pigmentation diseases and provide the missing knowledge needed to generate treatments and improve quality of life in patients with pigmentation diseases.

Table 1: Candidate novel melanosome proteins identified in Wyatt Beyer's TPC2 BioID experiment

Candidate Melanosome Proteins From TPC2 BioID Experiment	
Protein Name	**Abbreviation**
Leucine-Rich Melanocyte Differentiation-Associated Protein/ Oculocutaneous Albinism Type 7	LRMDA/OCA7
Myosin Heavy Chain 9/Myosin 2A	MYH9/Myo2A
Phospholipase D1	PLD1
Formin Like Protein 2	FMNL2
Myosin Heavy Chain 10/Myosin 2B	MYH10/Myo2B
Synaptic Vesicle Glycoprotein 2A	SV2A
Tetraspanin-10	TSPAN10
Cortactin	CTTN

Experimental Approach

To test if the candidate proteins identified from the TPC2 BioID experiment are involved in the pigmentation process, small interfering RNA (siRNA) was utilized to test for a pigmentation phenotype in cells with knocked down level of the candidate protein (Table 2). A human melanoma cell line, MNT1 cells, which are the standard for studying melanocytes were used for all experiments. Due to the pigmented nature of the MNT1 cells, brightfield microscopy can be used to gain information about pigmentation levels in cells. After transfecting and growing wild type cells with siRNA control or siRNA against the protein of interest, total cell extracts were analyzed by western blotting to confirm that the candidate protein was successfully knocked down (Table 3). Once the knockdown was confirmed via western blot, cells were fixed, immunostained with antibodies to the protein subject to knockdown and

analyzed by light microscopy in a double-blind manner to ensure no bias. Widefield fluorescent images were used to further confirm knockdown success and brightfield images were processed and analyzed by two methods to screen for a pigmentation phenotype. The first method was measuring integrated density which provides measurements of darkness per cell. The second method was percent cell area with pigment. These measurements will both show if knocking down the candidate protein causes a hypopigmented or hyperpigmented phenotype. siRNA knockdown cell lysates were also analyzed for a change in melanin producing enzymes tyrosinase or PMEL via western blots to test for a change in expression levels. In addition to looking for a phenotype, confocal fluorescent microscopy was used to check if the candidate proteins are localized to melanosomes using TPC2-EGFP as a fluorescent melanosome membrane marker.

If a strong phenotype was seen (Table 4), CRISPR-Cas9 was used to make knockout cell lines. In these cell lines, the fluorescent and brightfield microscopy was performed. Next, a rescue experiment was done to confirm the phenotype was due to the knockout of the candidate protein and not an off-target effect. A spectrophotometric melanin quantification assay was also used to determine if melanin content per cell changes in cell extracts from knockout cells. GraphPad Prism was used for all statistical analysis. Sample distribution normality was determined using the Shapiro-Wilk test. For parametric distributions (western blot analysis and spectrophotometric melanin quantification) a Student's T Test was performed and for nonparametric distributions (microscopy analysis) a Mann-Whitney Test was performed. Throughout this process, candidate proteins were screened for their involvement in pigmentation and a phenotype was confirmed. Further investigation will be needed to determine the mechanistic role identified proteins are playing in pigmentation.

Table 2: List of siRNAs used to make knockdown cells

siRNA	Purchased From	siRNA ID
siMock	ThermoFisher Scientific	4390844
siFMNL2-1	ThermoFisher Scientific	s41619
siFMNL2-2	ThermoFisher Scientific	s41620
siSV2A-1	ThermoFisher Scientific	s19183
siSV2A-2	ThermoFisher Scientific	s19184
siCTTN-1	ThermoFisher Scientific	s4665
siCTTN-2	ThermoFisher Scientific	n345340
siCTTN-3	ThermoFisher Scientific	s4666
siMYH9-1	ThermoFisher Scientific	s222
siMYH9-2	Gifted from O'Neil Wiggan	
siMYH9-3	ThermoFisher Scientific	s223
siMYH10-1	ThermoFisher Scientific	s9169
siMYH10-2	ThermoFisher Scientific	s9170
siMYH10-3	Gifted from O'Neil Wiggan	
siPLD1	ThermoFisher Scientific	s10637
siTSPAN10-1	ThermoFisher Scientific	s38272
siTSPAN10-2	ThermoFisher Scientific	s195449
siTSPAN10-3	ThermoFisher Scientific	s195448

Table 3: List of antibodies used for western blotting and immunofluorescence

Anti-	Clonality	Species	Company	Catalog Number	Dilution used for Western Blots
Formin Like Protein 2 (FMNL2)	Polyclonal	Mouse	abcam	ab5763	1:1000
Synaptic Vesicle Glycoprotein 2A (SV2A)	Monoclonal	Mouse	Developmental Studies Hybridoma Bank (DSHB)	SV2-c	1:1000
Cortactin (CTTN)	Monoclonal	Mouse	Millipore Sigma	05-180, clone 4F11	1:1000
Myosin Heavy Chain 9/ Myosin 2A (MYH9)	Polyclonal	Rabbit	Sigma-Aldrich	M8064	1:1500
Myosin Heavy Chain 10/ Myosin 2B (MYH10)	Polyclonal	Rabbit	Sigma-Aldrich	M7939	1:1500
Phospholipase D1 (PLD1)	Monoclonal	Mouse	Santa Cruz Biotechnology	sc-28314	1:500
Tetraspanin-10 (TSPAN10)	Polyclonal	Rabbit	Proteintech	14430-1-AP	1:1000
Tyrosinase (Tyr)	Monoclonal	Mouse	Santa Cruz Biotechnology	sc-20035	1:1000
HMB45 (PMEL17)	Monoclonal	Mouse	Dako	GA052	1:1000
GAPDH	Monoclonal	Mouse	Proteintech	60004-1-Ig	1:600,000

Table 4: Results of siRNA knockdown experiments and confocal microscopy experiment

Protein	Knockdown Successful?	Integrated Density (Darkness Per Cell)	Percent Cell Area with Pigment	Colocalize with TPC2
Tetraspanin-10 (TSPAN10)	Yes	Significant Decrease	Significant Decrease	Yes
Phospholipase D1 (PLD1)	Yes	Significant Decrease	Significant Decrease	Yes
Myosin Heavy Chain 10/ Myosin 2B (MYH10)	Yes	Significant Decrease	Significant Decrease	No
Myosin Heavy Chain 9/ Myosin 2A (MYH9)	Yes	Significant Decrease	Significant Decrease	No
Synaptic Vesicle Glycoprotein 2A (SV2A)	Yes	No Change	No Change	Yes
Formin Like Protein 2 (FMNL2)	Yes	No Change	No Change	No
Cortactin (CTTN)	Yes	No Change	No Change	No

CHAPTER 2: TETRASPANIN 10 (TSPAN10)

Background

Tetraspanin 10 (TSPAN10) is a poorly characterized four-pass transmembrane protein which belongs to the C8 family of tetraspanins (TSPANC8)[18]. These tetraspanins have 8 cysteine residues which are conserved across the whole family of proteins[18]. There is approximately 26% to 78% amino acid conservation amongst sequences of the various tetraspanins within the family[18]. The TSPAN10 amino acid sequence ranges from 26.3% conserved when compared to TSPAN15 to 34.5% conserved when compared with TSPAN5[18]. TSPANC8s are known to be chaperones in the trafficking of the protease ADAM10 from the ER through the Golgi and to its target membrane[19]. Tetraspanins 5, 14, 15, 17, and 33 traffic ADAM10 to the plasma membrane[19–21]. Interestingly, published data suggests TSPAN10 traffics ADAM10 to intracellular compartments[19–21]. ADAM10 is a protease known to be critical for the cleavage of many cell signaling enzymes and has been shown to be a protease involved in the cleavage of PMEL in the process of melanosome biogenesis[22].

In addition to the above link to melanosome biogenesis, other tetraspanins are known to be critical for proper melanosome biogenesis. For example, the tetraspanin CD63 is involved in the formation of intraluminal vesicles and sorting of PMEL onto intraluminal vesicles and is critical for proper PMEL fibril formation and early stages of melanosome biogenesis[23].

Tetraspanin 10 was discovered in the TPC2 BioID experiment indicating that it is in the proximity of melanosomes or physically at melanosomes. It may be playing a similar role to CD63 or be trafficking ADAM10 to the forming melanosomes. These hypothesizes as well as

the indication that it is in the proximity of melanosomes from the BioID screening made TSPAN10 a very promising potential melanosome protein.

Results

Three siRNAs targeting different regions of the TSPAN10 mRNA were used to generate three sets of TSPAN10 knockdown cells. The success of all three knockdowns was confirmed by western blotting and two knockdowns were confirmed by immunofluorescent staining of TSPAN10 (Figure 1). In the brightfield imaging both darkness per cell and cell area with pigment showed a subtle but statistically significant hypopigmented phenotype in the knockdown cells (Figure 2). TSPAN10 also had a high level of colocalization with TPC2 in preliminary confocal fluorescence microscopy experiments indicating it is at melanosome membranes (Figure 3B). While PMEL expression did not appear consistently changed in RIPA lysate samples (Figure 3A), this does not confirm a PMEL phenotype is not present in the knockdown cells. PMEL has an insoluble unprocessed fragment which is lost during the RIPA lysate production process.

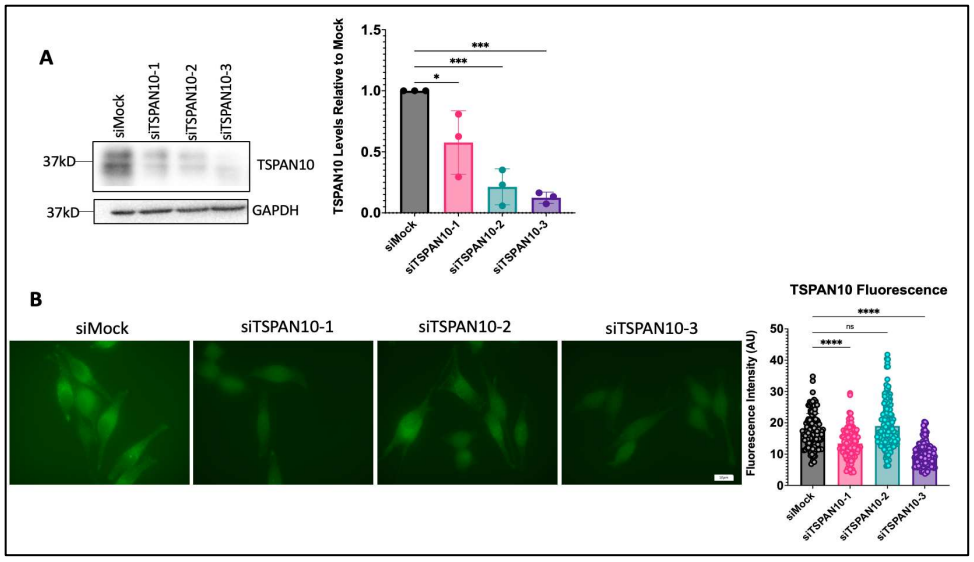

Figure 1: (A) Western blot demonstrating successful knockdown of TSPAN10 and corresponding quantification for 3 biological replicates. **(B)** Representative widefield fluorescence microscopy images of MNT1 cells transfected with siRNA and immunostained against TSPAN10 and corresponding fluorescence intensity quantification (siMock n=121, siTSPAN10-1 n=117, siTSPAN10-2 n=166, siTSPAN10-3 n=167) ($10\mu m$ *scale bar*).

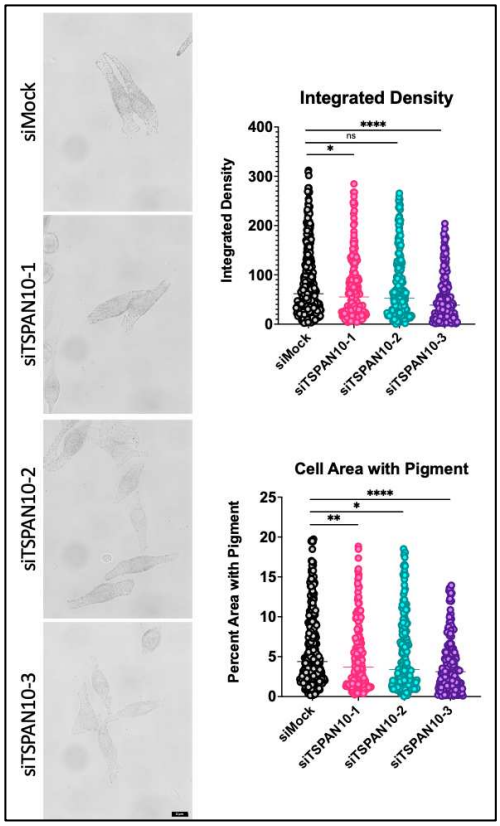

Figure 2: Representative brightfield images and corresponding quantification for integrated density (darkness per cell) and cell area with pigment (siMock n=97, siTSPAN10-1 n=88, siTSPAN10-2 n=131, and siTSPAN10-3 n=141) (10μm *scale bar*).

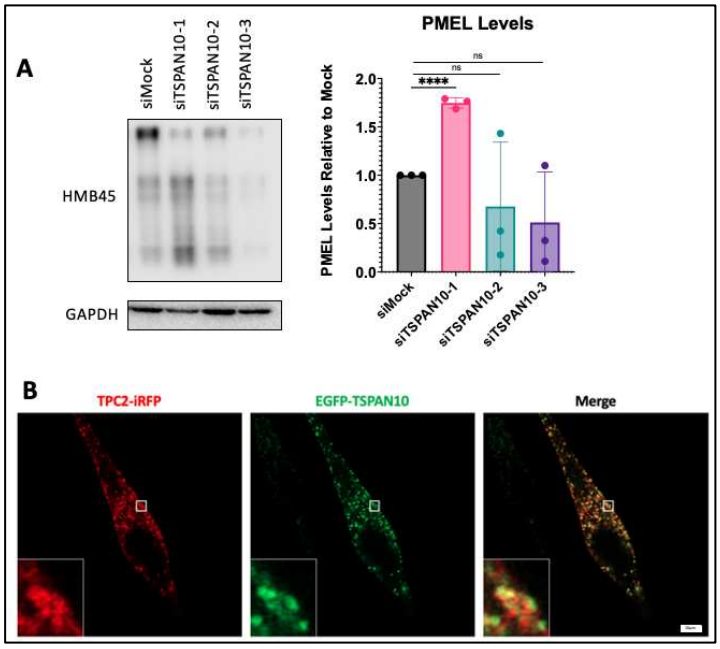

Figure 3: (A) Western blot of PMEL (HMB45) in total cell extracts from siRNA knockdown cells and corresponding quantification for 3 biological replicates. **(B)** Representative image of confocal fluorescence microscopy for exogenously expressed TSPAN10-EGFP (green) colocalization with exogenously expressed TPC2-iRFP (red) experiment (10μm *scale bar*).

Based on the colocalization and brightfield indicating that TSPAN10 is involved in pigmentation and at melanosomes, CRISPR-Cas9 was used to generate TSPAN10 knockout MNT1 cells. The success of the knockout was confirmed by western blotting and immunofluorescent staining of TPSAN10 (Figure 4). The brightfield image analysis was also carried out within these cells and a more drastic hypopigmented phenotype was seen in the knockout cells (Figure 5A). This may be due to residual TSPAN10 in siRNA treated cells compared to knockout cells. In addition, the amount of melanin per cell quantified by spectrophotometric methods was decreased in the TSPAN10 knockout cell lines (Figure 5B).

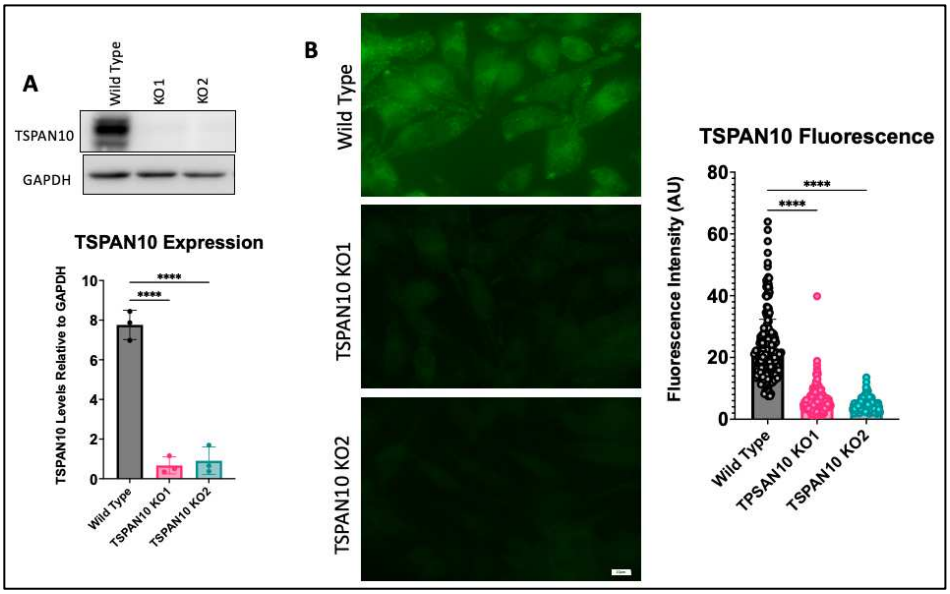

Figure 4: (A) Western blot demonstrating successful knockout of TSPAN10 and corresponding quantification for 3 biological replicates of the CRISPR-Cas9 knockout cell lysates. **(B)** Representative widefield fluorescence microscopy images of MNT1 TSPAN10 knockout cells immunostained against TSPAN10 and corresponding fluorescence intensity quantification (Wild Type n=242, TSPAN10 KO1 n=258, and TSPAN10 KO2 n=178) ($10\mu m\ scale\ bar$).

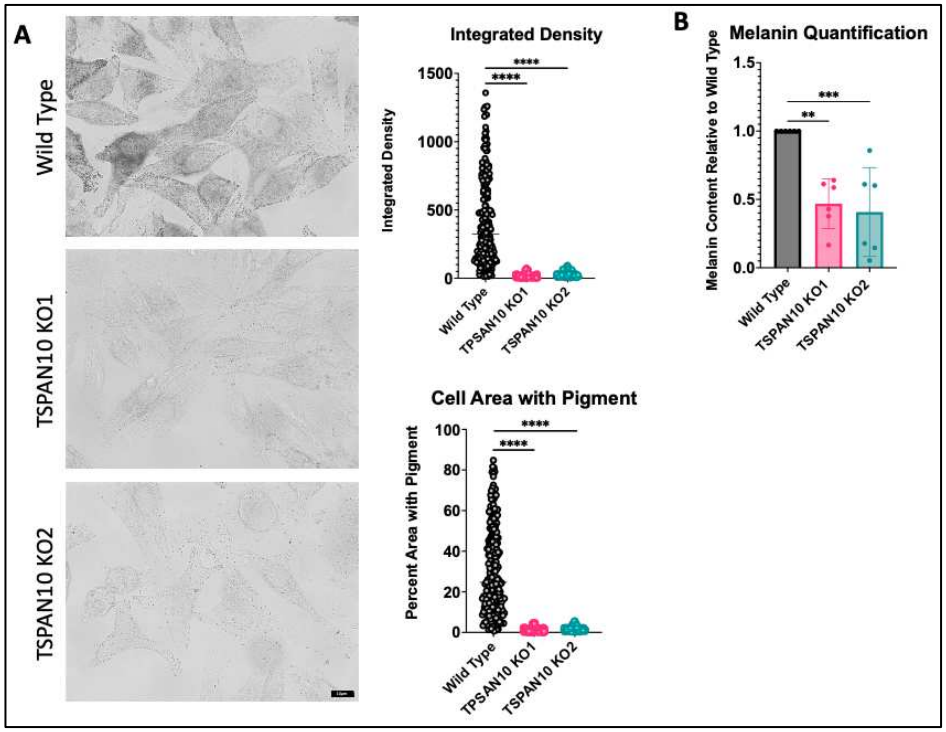

Figure 5: (A) Representative brightfield images and corresponding quantification for integrated density (darkness per cell) and cell area with pigment (Wild Type n=241, TSPAN10 KO1 n=212, and TSPAN10 KO2 n=155). **(B)** Melanin content per cell in three biological replicates of wild type and TSPAN10 knockout cells ($10\mu m\ scale\ bar$).

When TSPAN10-EGFP was overexpressed in the knockout cells, pigmentation was restored to above normal levels (Figure 6). This ability to rescue pigmentation by reintroducing TSPAN10, demonstrates that the hypopigmentation phenotype seen is due to lack of TSPAN10 and not an off-target effect of the siRNA or CRISPR. This also suggests the overexpression of TSPAN10 caused increased pigmentation. To confirm this, TSPAN10-EGFP was overexpressed in wild type MNT1 cells. The wild type cells overexpressing TSPAN10 had a significant increase in pigmentation (Figure 7), providing further evidence that TSPAN10 is a key player in regulating pigmentation levels.

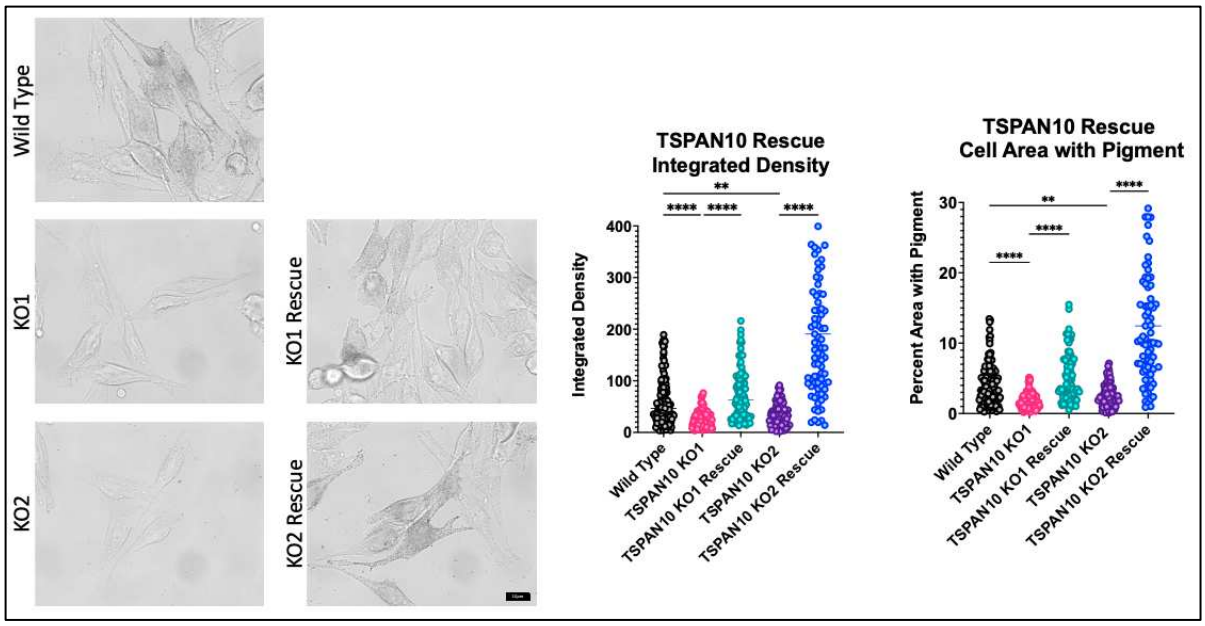

Figure 6: Representative brightfield images and corresponding quantification for integrated density (darkness per cell) and cell area with pigment in wild type cells expressing EGFP, TSPAN10 KO1 cells expressing EGFP, TSPAN10 KO1 cells expressing TSPAN10-EGFP, TSPAN10 KO2 cells expressing EGFP, and TSPAN10 KO2 cells expressing TSPAN10-EGFP (Wild Type n=137, TSPAN10 KO1 n=119, TSPAN10 KO1 rescue n=79, TSPAN10 KO2 n=92, and TSPAN10 KO2 rescue n=93) ($10\mu m$ *scale bar*).

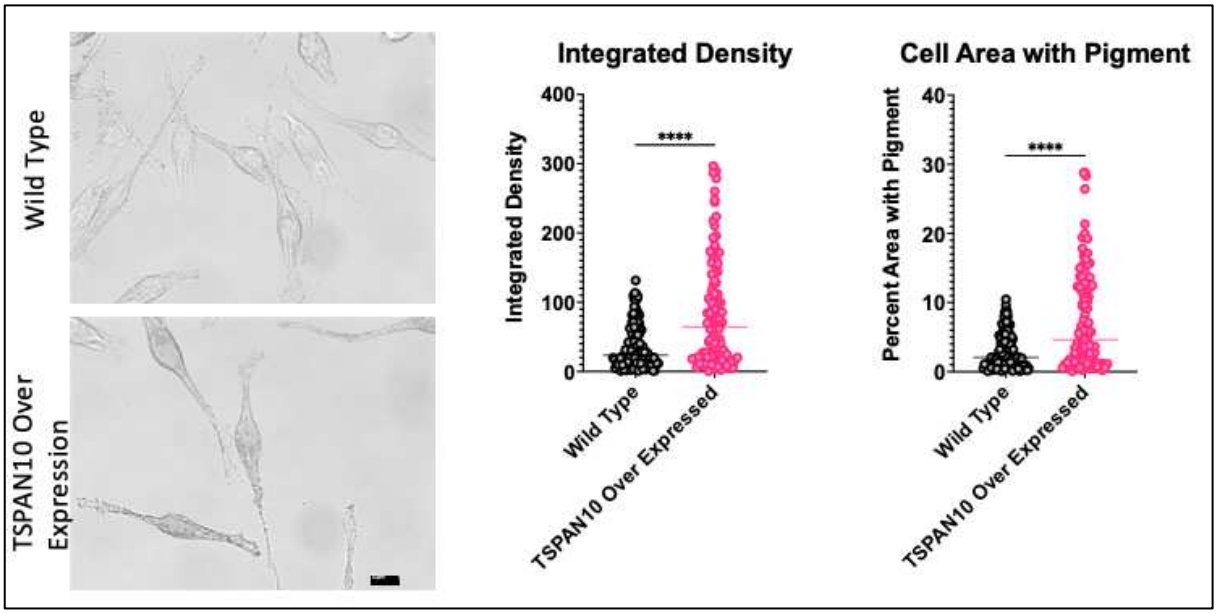

Figure 7: Representative brightfield images and corresponding quantification for integrated density (darkness per cell) and cell area with pigment in wild type cells expressing EGFP or TSPAN10-EGFP (Wild Type n=127 and TSPAN10 over expressed n=102) (10μm *scale bar*).

Discussion

Knocking down and knocking out TSPAN10 in melanocytes lead to a hypopigmented phenotype, and overexpressing TSPAN10 lead to a hyperpigmented phenotype. TSPAN10 localizes to melanosomes (Table 4). Based on what is known about TSPAN10 and the known roles of tetraspanins in melanosome biogenesis, lack of TSPAN10 in melanocytes may cause melanosome biogenesis to occur improperly leading to the observed hypopigmented phenotype. When TSPAN10 is not present in melanocytes, the PMEL containing intralumenal vesicles characteristic of stage 1 melanosomes may have a defect, like what is seen in melanocytes lacking CD63. Another possible explanation for the hypopigmentation in cells lacking TSPAN10, is when TSPAN10 is not present then ADAM10 is not being trafficked properly and PMEL is not being cleaved properly.

While the mechanism that TSPAN10 plays in melanocytes has not been investigated yet, it will be in the near future. A good starting place for investigating the mechanism is to look for a

PMEL processing defect. To do this, western blots should be run on Triton-X100 soluble and insoluble samples from wild type and knockout cells with various PMEL antibodies. Electron microscopy should also be performed to determine if there is a change in the number of melanosomes at different stages of biogenesis or if any PMEL defects can be observed. Based on the results of this step, many follow up experiments can be done to determine if TSPAN10 is functioning like CD63, if ADAM10 is mis-trafficked, or if the hypopigmented phenotype is due to a different mechanism. Three examples of these follow up experiments are: to test if ADAM10 is at melanosomes and colocalizes with TSPAN10, to determine if ADAM10 is mis-trafficked in TSPAN10 knockout cells, and to check if a pigmentation phenotype occurs in cells treated with an ADAM10 inhibitor. These three experiments will help determine if the phenotype is due to TSPAN10's known role with ADAM10 or if it is because of a different function of TSPAN10.

TSPAN10 has been shown to be a protein necessary for pigmentation. Future investigation into its mechanism and involvement with melanosomes will provide a deeper understanding of the pigmentation process. TSPAN10's characterization may answer questions about pigmentation diseases or lead to the discovery of other novel melanosome proteins.

CHAPTER 3: FORMIN LIKE PROTEIN 2 (FMNL2)

Background

Formins are a critical element of cytoskeleton regulation. They are Rho GTPase effector proteins known to function as actin nucleator proteins involved in the formation of linear actin filaments[24,25]. Emerging evidence suggests that formins also regulate microtubule dynamics in an actin independent way[26]. Diaphanous-related formins (DRFs) are the most well characterized family of formins, which includes formin like proteins. Formin like protein 2 (FMNL2) has been linked to the invasive ability of colorectal[27]and melanoma cancer cells[28] as well as is a known key factor involved in some intellectual disabilities and primary ovarian insufficiency[29]. In addition, FMNL2 is known to regulate anterograde transport through the Golgi apparatus via interactions with Cdc42, a Rho GTPase[30]. Cdc42 is necessary for Golgi polarization and melanoblast movement in embryos[31]. FMNL2 mediated actin assembly is lost in cells lacking Cdc42[30] indicating that lack of proper FMNL2 function may be involved in the improper transport and melanoblast movement seen in embryos lacking Cdc42.

Actin and microtubules are known to be involved in melanosome transfer and movement; however, the role of formins or formin like proteins in skin pigmentation has not been investigated. FMNL2 was detected in the TPC2 BioID experiment indicating that it was in the proximity of melanosomes at some point during the experiment. The fact that formins are a key regulation factor of the cytoskeleton, in addition to the known importance of the cytoskeleton in skin pigmentation and melanosome transport, suggest that FMNL2 may be a key regulating protein of the cytoskeleton necessary for melanosome movement and transport. If FMNL2 is a

necessary protein involved in melanosome function, a pigmentation phenotype should be observed when FMNL2 is knocked down in cells.

Results

Two siRNAs targeting different regions of the FMNL2 mRNA were used to generate two sets of FMNL2 knockdown cells. The success of the knockdowns was confirmed by western blotting and immunofluorescent staining of FMNL2 (Figure 8). In the siRNA knockdown cells there was no change in darkness per cell or the percent cell area containing pigment (Figure 9).

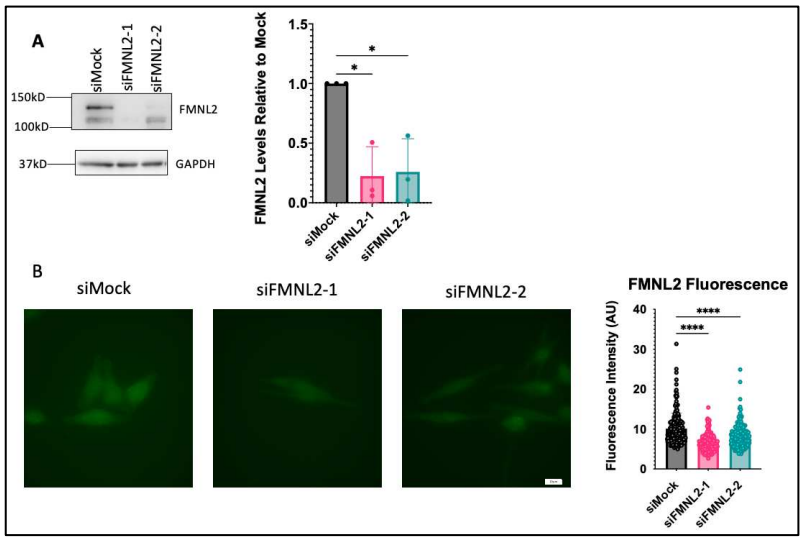

Figure 8: (A) Western blot demonstrating successful knockdown of FMNL2 and corresponding quantification for 3 biological replicates of siRNA transfected MNT1 cells. **(B)** Representative widefield fluorescence microscopy images of MNT1 cells transfected with siRNA and immunostained against FMNL2 and corresponding fluorescence intensity quantification (siMock n=208, siFMNL2-1 n=208, and siFMNL2-2 n=268) (10μm *scale bar*).

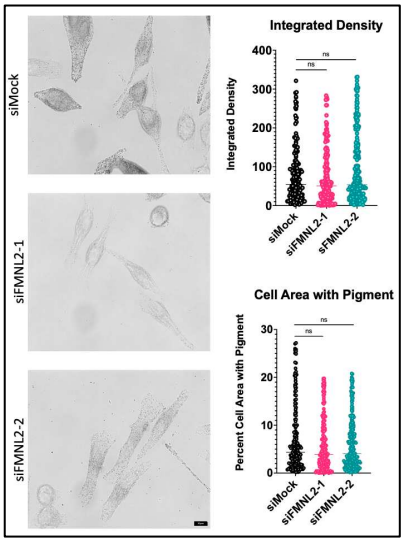

Figure 9: Representative brightfield images and corresponding quantification for integrated density (darkness per cell) and cell area with pigment (siMock n=169, siFMNL2-1 n=184, and siFMNL2-2 n=240) (10μm *scale bar*).

This indicates that FMNL2 is not necessary for proper cell pigmentation. In addition, there was not a consistent change in the expression of melanosome biogenesis enzymes tyrosinase or PMEL in knockdown cell lysates (Figure 10A). The siFMNL2-2 knockdown cell lysates did have a slightly significant decrease in overall PMEL expression; however, because of a lack of an associated pigmentation phenotype, this decrease was most likely due to limitations in the method used. PMEL has an insoluble, unprocessed fragment which is lost in the process of making a RIPA buffer extract lysate. This loss can potentially explain the slight PMEL level

decrease seen in the knockdown cells. FMNL2 also did not appear to colocalize with TPC2 in a preliminary colocalization experiment indicating that it is not at melanosomes (Figure 10B).

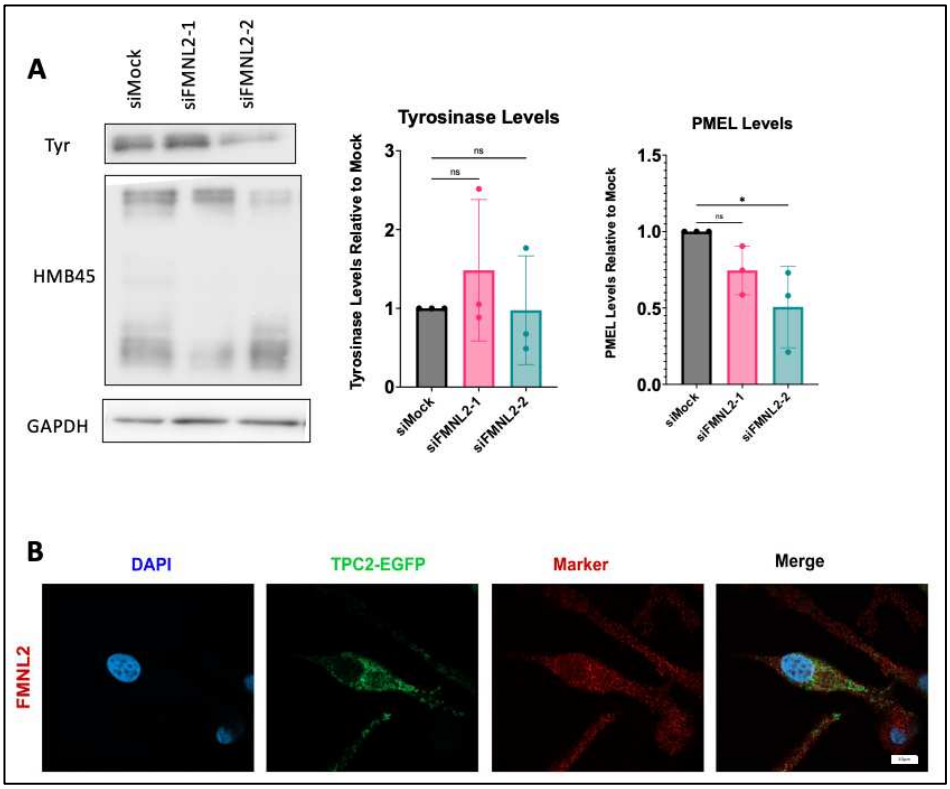

Figure 10: (A) Western blot of tyrosinase (Tyr) and PMEL (HMB45) in total cell extracts from siRNA knockdown cells and corresponding quantification for 3 biological replicates. **(B)** Representative image of confocal fluorescent microscopy for immunostained FMNL2 (red) colocalization with exogenously expressed TPC2-EGFP (green) experiment ($10\mu m\ scale\ bar$).

Discussion

Knocking down FMNL2 did not produce a pigmentation phenotype (Table 4). This suggested that FMNL2 is not necessary for proper melanosome biogenesis and function. Based on the TPC2 BioID experiment, FMNL2 is in the proximity of melanosomes but it may not be interacting with melanosomes, or it may not be necessary for proper pigmentation due to redundancy. Other formins or formin like proteins may be compensating when FMNL2 is knocked down. To further investigate the role of FMNL2, other formins may need to be knocked down in combination with FMNL2. Alternatively, FMNL2 may be needed for the downstream process of melanosome transfer to keratinocyte, which was not assessed here. Since FMNL2 did

not give a pigmentation phenotype its involvement in melanocyte related pigmentation was not further investigated.

CHAPTER 4: SYNAPTIC VESICLE GLYCOPROTEIN 2A (SV2A)

Background

Synaptic vesicle glycoprotein 2A (SV2A) is a twelve-pass transmembrane protein known to be found at synapses of all neurons[32]. Evidence shows that SV2A may regulate synaptic exocytosis via regulating the calcium sensor synaptotagmin-1 and emerging evidence indicates it may be a vesicle transporter[32]. While the mechanistic function of SV2A is still being characterized, it is known to be a key protein lost in many neurodegenerative diseases including Alzheimer's Disease, Huntington's Disease, and Epilepsy[33–35]. In addition to being linked to diseases, it is currently being studied as a potential treatment for Epilepsy[36] and studied as a potential detection technique for Alzheimer's Disease[35]. SV2A has predominately been studied in neurons, so very little is known about its expression or function in other cell types.

SV2A was detected in the TPC2 BioID experiment indicating that it is in the proximity of melanosomes and is expressed in MNT1 cells. Synaptotagmin-1 is not known to function in melanocytes; however, a different synaptotagmin, synaptotagmin-4, has been reported to promote melanogenesis in alpaca melanocytes[37]. This link between synaptotagmin and pigmentation suggests that synaptotagmins may be involved in melanogenesis in human melanocytes. The known function of SV2A in the regulation of synptotagmin-1 and vesicle movement, makes it a potential candidate protein involved in melanosome movements and the passage of melanin to neighboring keratinocytes. While the exact mechanism of how melanin is passed to keratinocytes is unknown, one hypothesis is that the melanosome membrane fuses with the plasma membrane releasing the melanin to the extracellular space to be endocytosed by the keratinocyte. This membrane fusion could potentially involve SV2A. If SV2A is necessary for

membrane fusion, a pigmentation phenotype may be seen when SV2A is knocked down due to melanin not being released from the melanocyte. If SV2A is involved in vesicle transport, either a hypopigmented or hyperpigmented phenotype may occur.

Results

Two siRNAs targeting different regions of the SV2A mRNA were used to create two sets of SV2A knockdown cells and the knockdown success was confirmed via immunofluorescence microscopy of SV2A (Figure 11). In these SV2A knockdown cells, there was no change in darkness per cell or cell area containing pigment (Figure 12). There was also no change in the expression of tyrosinase or PMEL (Figure 13A). Interestingly, SV2A appeared to have a high level of colocalization with TPC2 in preliminary colocalization experiments indicating that it is at melanosomes membranes (Figure 13B).

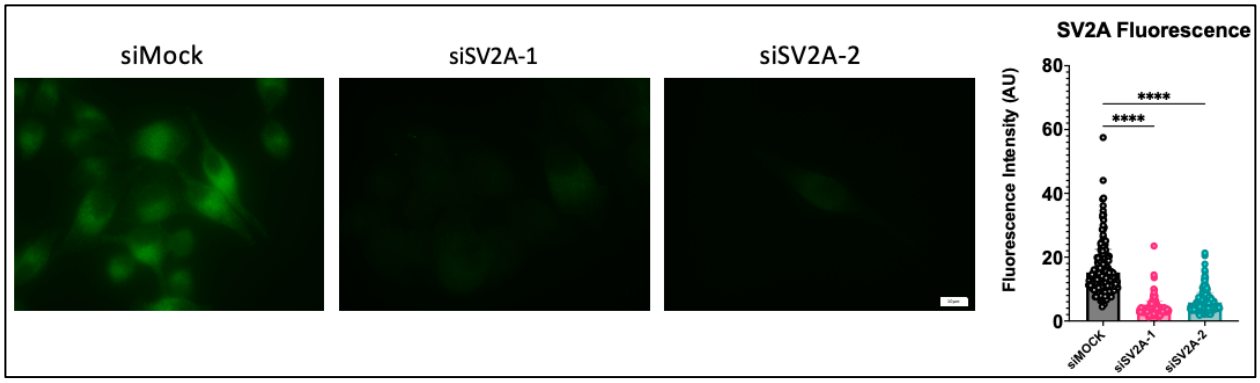

Figure 11: Representative widefield fluorescence microscopy images of MNT1 cells transfected with siRNA and immunostained against SV2A and corresponding fluorescence intensity quantification (siMock n=225, siSV2A-1 n=208, and siSV2A-2 n=242) (10μm *scale bar*).

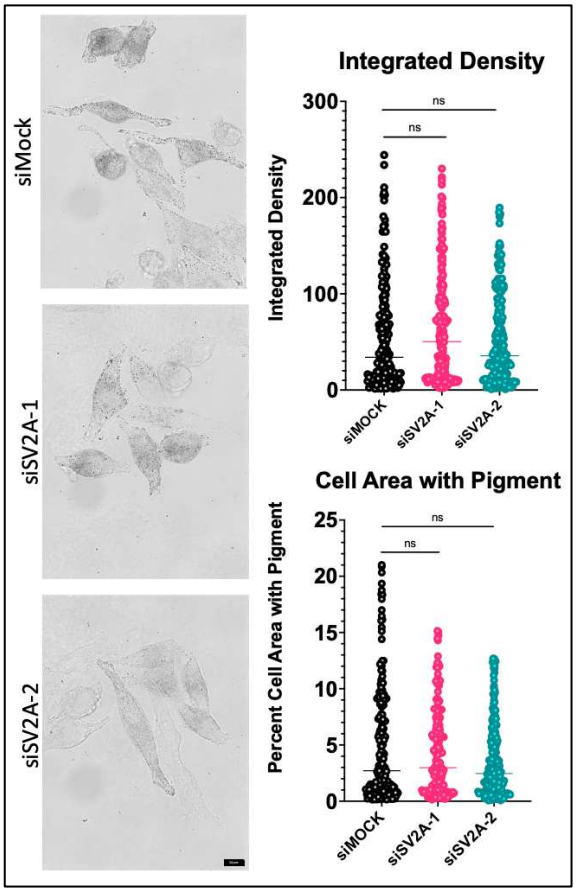

Figure 12: Representative brightfield images and corresponding quantification for integrated density (darkness per cell) and cell area with pigment (siMock n=185, siSV2A-1 n=178, and siSV2A-2 n=219) (10μm *scale bar*).

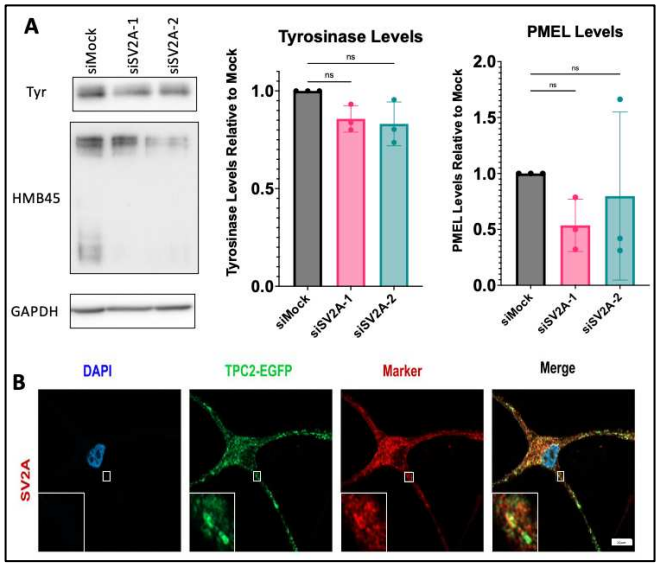

Figure 13: (A) Western blot of tyrosinase (Tyr) and PMEL (HMB45) in total cell extracts from siRNA knockdown cells and corresponding quantification for 3 biological replicates. **(B)** Representative image of confocal fluorescent microscopy for immunostained SV2A (red) colocalization with exogenously expressed TPC2-EGFP (green) experiment (10μm *scale bar*).

Discussion

SV2A is in melanocytes and at melanosomes as discovered through the TPC2 BioID and the colocalization of SV2A with TPC2; however, it does not appear to be necessary for proper pigmentation production (Table 4). If SV2A was critical for pigmentation, a phenotype would have been observed when the protein was knocked down. While SV2A did not show a pigmentation phenotype when knocked down, it appeared to localize to melanosomes. The localization of SV2A to melanosomes suggests that SV2A may be functioning at melanosomes in a way which is unrelated to pigmentation or that knocking down the protein may cause a phenotype which the methods used are not sensitive enough to detect. Alternatively, SV2A may be involved in melanin exocytosis, which would necessitate co-culture with the keratinocyte for

proper testing of this potential function. To further investigate the role of SV2A in melanocytes, CRISPR-Cas9 knockout cell lines are currently being developed.

CHAPTER 5: CORTACTIN (CTTN)

Background

Cortactin (CTTN) is known to be expressed in many cell types and to be a key regulator in various cell processes[38]. It is involved in processes ranging from endocytosis to cell migration. Its function is dependent upon its interaction with the actin network at the cell cortex and various organelles and its role as a branched actin regulator[38,39]. CTTN is tightly regulated by its phosphorylation status[39] and its overexpression is believed to be a key factor in cancer cell invasion[40]. Emerging evidence suggests that CTTN is involved in the regulation of endosomal trafficking and vesicle transport[41].

CTTN is known to be localized to sites of constriction and fission of tubules emanating from melanosomes as well as melanosome movement[42]. While melanin transfer to keratinocytes is not fully characterized, most evidence suggests that melanosomes move on microtubules and then are transferred to actin near the plasma membrane at melanocyte dendrite tips. Some studies, however, suggest actin is the main melanosome transport method throughout the melanocyte[6,42].

CTTN was detected in the TPC2 BioID experiment suggesting that it is in the proximity of melanosomes. Based on the known involvement of actin at melanocyte dendrite tips and the key actin regulation via CTTN, it seemed likely that CTTN could be functioning in pigmentation via regulation of actin utilized in melanosome transport. If CTTN is involved in pigmentation, MNT1 cells which have CTTN knocked down with siRNA will have an improper actin network causing mis-trafficking of melanosome cargos or the melanosomes themselves. This mis-trafficking may cause a hypopigmented or hyperpigmented phenotype depending on how the

mis-trafficking occurs. The melanosomes may just remain in the cell and accumulate causing a hyperpigmented phenotype or they may be degraded by lysosomes or released from the cell via exocytosis causing a hypopigmented phenotype. In addition if melanosome cargo is mis-trafficked, melanosome biogenesis defects may occur leading to a hypopigmented phenotype.

Results

Three siRNAs targeting different regions of the CTTN mRNA were used to make three sets of CTTN knockdown cells. The success of the knockdowns was confirmed by western blotting and immunofluorescent staining of CTTN (Figure 14). siCTTN-3 gave the strongest knockdown based on both methods of checking (Figure 14). When brightfield imaging analysis of the knockdown cells was preformed, siCTTN-1 gave a significant decrease in pigmentation; however, the other two siRNAs did not show a phenotype (Figure 15). Since the result from siCTTN-1 was not reproducible with other siRNAs against CTTN, siCTTN-1 was probably having an off-target effect, and the phenotype observed was not truly due to the knockdown of CTTN. In addition, tyrosinase and PMEL expression was not affected by the knockdown of

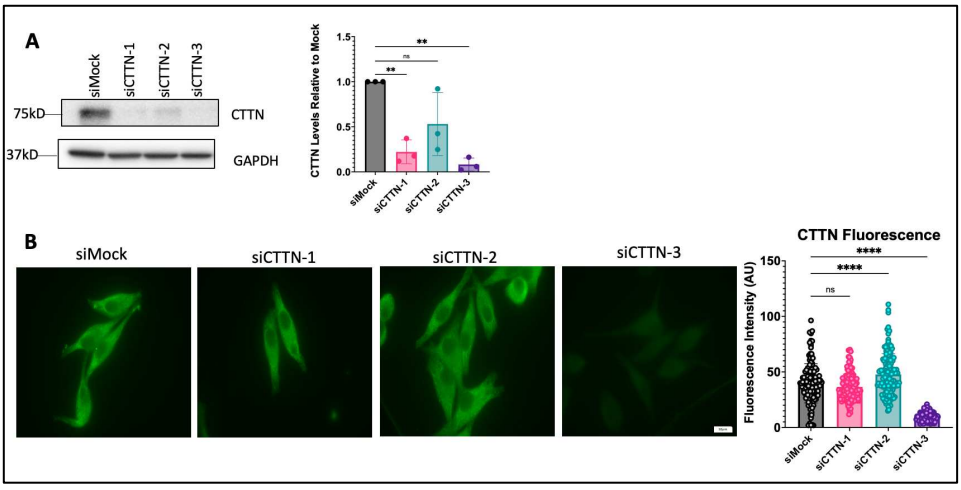

Figure 14: (A) Western blot demonstrating successful knockdown of CTTN and corresponding quantification for 3 biological replicates. **(B)** Representative widefield fluorescent microscopy images of MNT1 cells transfected with siRNA and immunostained against CTTN and corresponding fluorescence intensity quantification (siMock n=135, siCTTN-1 n=187, siCTTN-2 n=152, and siCTTN-3 n=217) ($10\mu m$ *scale bar*).

CTTN and CTTN did not appear to colocalize significantly with TPC2 in preliminary experiments (Figure 16).

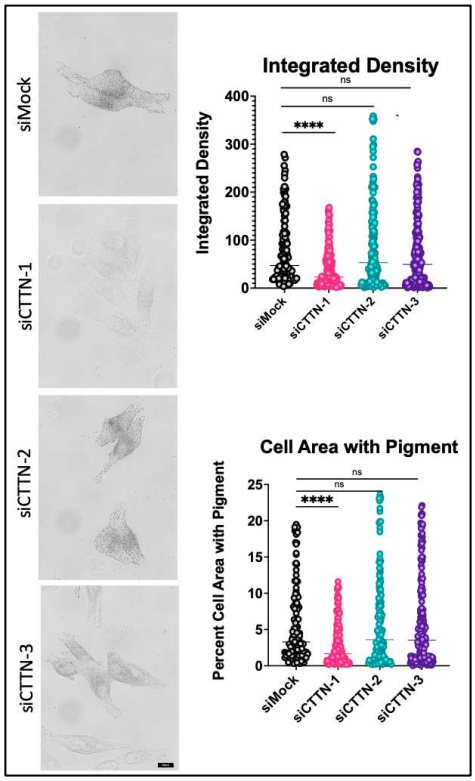

Figure 15: Representative brightfield images and corresponding quantification for integrated density (darkness per cell) and cell area with pigment (siMock n=120, siCTTN-1 n=162, siCTTN-2 n=143, and siCTTN-3 n=194) (10μm *scale bar*).

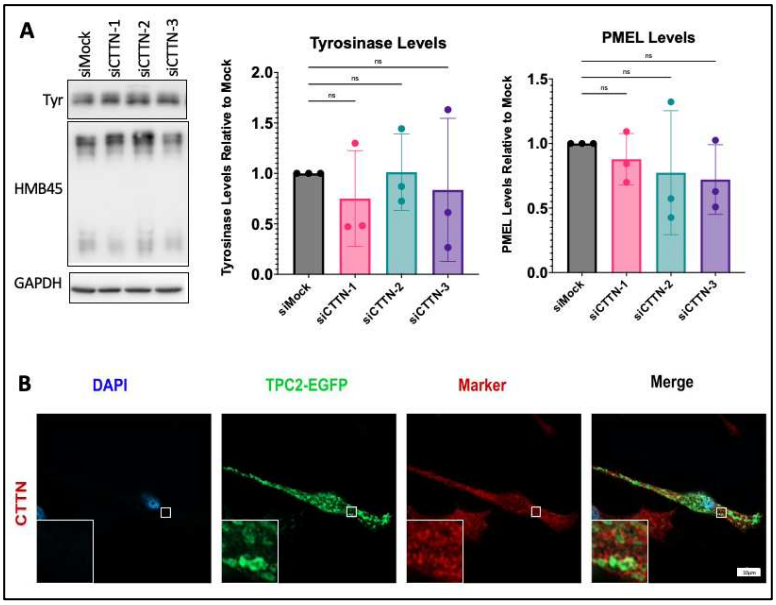

Figure 16: (A) Western blot of tyrosinase (Tyr) and PMEL (HMB45) in total cell extracts from siRNA knockdown cells and corresponding quantification for 3 biological replicates. **(B)** Representative image of confocal fluorescent microscopy for immunostained CTTN (red) colocalization with exogenously expressed TPC2-EGFP (green) experiment (10μm *scale bar*).

Discussion

The lack of a consistent phenotype suggests that CTTN is not playing a critical role in pigmentation. While CTTN may be in the proximity of melanosomes, it may be involved in a different cellular function. Alternatively, CTTN may have been interacting with actin at the melanosome but CTTN itself may not be required for melanosome biogenesis or transport. To understand why CTTN was detected in the proximity of melanosomes, more experiments are needed.

CHAPTER 6: MYOSIN HEAVY CHAIN 9 (MYH9) AND MYOSIN HEAVY CHAIN 10 (MYH10)

Background

Myosins are cellular motors that walk along actin. They are critical for many cellular processes including muscle contraction, vesicle movement and cell division. Myosin heavy chain 9 (MYH9), also known as Non-Muscle Myosin II A, has been linked to many human diseases including hearing loss, macrothrombocytopenia, and glomerulonephritis[43–45]. Myosin heavy chain 10 (MYH10), also known as Non-Muscle Myosin II B, has been linked to megakaryocyte polyploidization, hepatocellular carcinoma metastasis, and pulmonary disease[46–49]. MYH9 and MYH10 are known to be expressed in many cell types and thought to be isoforms which self-assemble into filaments and control cell protrusions and cell adherence via actin crosslinking and contraction, however, their exact functions in melanocytes have yet to be investigated.

While melanosome movement and transfer are not fully characterized, certain myosins are well characterized key players in this process[50–52]. Myosin 5c has been shown to be involved in melanosome biogenesis and secretion in melanocytes[53], and myosin 7a is well characterized in the transport of melanosomes in retinal pigmented epithelium cells[54]. Myosin 7a has been linked to skin pigmentation via a genome-wide mouse reverse genetic screening[55], and MYH9 is known to physically interact with myosin 7a[45]. This interaction as well as the link to myosin 7a being in melanocytes, and MYH9 being detected in the proximity of melanosomes via the BioID experiment, made it a promising candidate melanosome protein. MYH10 interacts with and co-localizes with MYH9 in many cell-types[56], so it is probable that MHY10 and MYH9 may colocalize and have overlapping function in melanocytes. It is hypothesized that MYH9 and MYH10 are at melanosome membranes, playing a key role in melanosome biogenesis by aiding

in the constriction of tubules transporting biogenesis cargo from the endosome to the forming melanosome or in tubules recycling cargo from the melanosome back to the endosome. If these myosins are involved in melanosome biogenesis, when the myosins are knocked down the melanosomes would be expected to have melanosome biogenesis defects leading to a hypopigmented phenotype.

Results

Three siRNAs targeting different regions of the MYH9 mRNA were used to generate three sets of siMYH9 cells and three siRNAs targeting different regions of the MYH10 mRNA were used to generate three sets of siMYH10 cells. MYH9 appeared to be successfully knocked down with the three siRNAs via western blot (Figure 17A); however, siMYH9-2 knockdown success could not be confirmed via immunostaining against MYH9 (Figure 17B). siMYH9-2 cells appeared to have an increase in MYH9 fluorescence which is the opposite of what should be observed if MYH9 was successfully knocked down (Figure 17B). The success of two MYH10 knockdowns was confirmed by western blotting and immunofluorescent staining of MYH10 with the third siRNA giving a non-significant decrease in MYH10 expression (Figure 18).

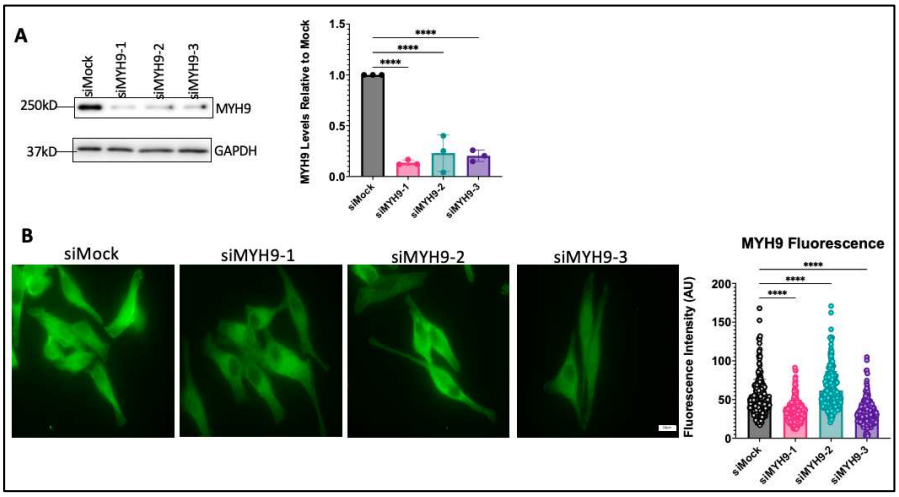

Figure 17: (A) Western blot demonstrating successful knockdown of MYH9 and corresponding quantification for 3 biological replicates. **(B)** Representative widefield fluorescent microscopy images of MNT1 cells transfected with siRNA and immunostained against MYH9 and corresponding fluorescence intensity quantification (siMock n=241, siMYH9-1 n=252, siMYH9-2 n=235, and siMYH9-3 n=225) ($10\mu m$ *scale bar*).

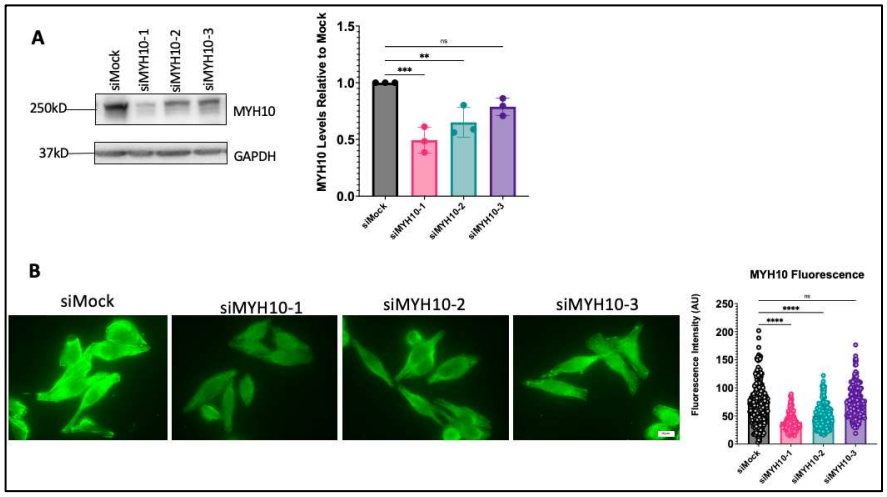

Figure 18: (A) Western blot demonstrating successful knockdown of MYH10 and corresponding quantification for 3 biological replicates. **(B)** Representative widefield fluorescent microscopy images of MNT1 cells transfected with siRNA and immunostained against MYH10 and corresponding fluorescence intensity quantification (siMock n=244, siMYH10-1 n=184, siMYH10-2 n=214, and siMYH10-3 n=183) ($10\mu m\ scale\ bar$).

For MYH9, two siMYH9 knockdown cell lines showed a hypopigmented phenotype while the other siMYH9 knockdown showed a hyperpigmented phenotype (Figure 19). For MYH10, all three knockdowns showed a hypopigmented phenotype (Figure 20).

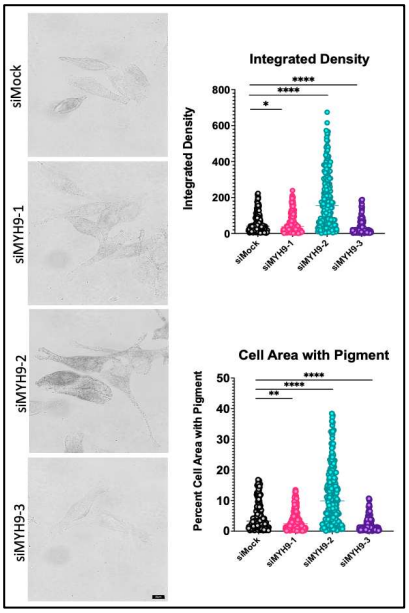

Figure 19: Representative brightfield images and corresponding quantification for integrated density (darkness per cell) and cell area with pigment (siMock n=212, siMYH9-1 n=217, siMYH9-2 n=217, and siMYH9-3 n=176) ($10\mu m\ scale\ bar$).

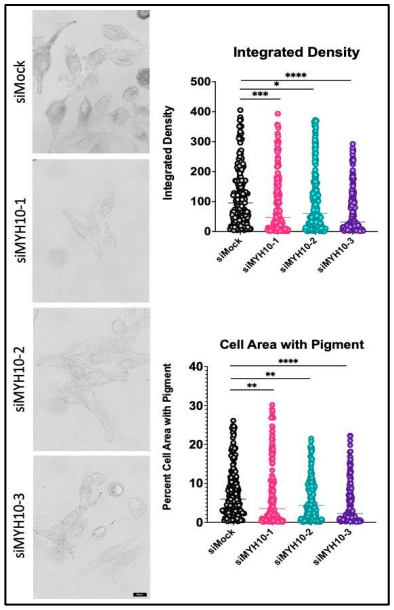

Figure 20: Representative brightfield images and corresponding quantification for integrated density (darkness per cell) and cell area with pigment (siMock n=205, siMYH10-1 n=163, siMYH10-2 n=188, and siMYH10-3 n=158) ($10\mu m\ scale\ \boldsymbol{bar}$).

Based off the myosins being isoforms of one another, their knockdown would be expected to give the same phenotype. The fluorescence result showing an unsuccessful knockdown of siMYH9-2 and the other two siMYH9 cells showing a different phenotype than siMYH9-2, indicate that the siRNA used to generate siMYH9-2 is possibly having an off-target effect. With the assumption that siMYH9-2 is giving off-target results, it can be concluded that both MYH9 and MYH10 knockdowns give a hypopigmented phenotype.

The knockdown of these myosins did not change the expression of tyrosinase or PMEL (Figure 21A and 22A). siMYH9-2 showed a decrease in PMEL; however, these cells showed a hyperpigmented phenotype (Figure 19 and 21A). If PMEL levels were truly decreased a hypopigmentation phenotype should have been seen and the PMEL decrease should have been observed in the other siMYH9 knockdown cells. This PMEL change further supports that there is an off-target effect of the siRNA in the siMYH9-2 cells. Interestingly, the proteins did not appear to significantly colocalize with TPC2 in preliminary experiments (Figure 21B and 22B).

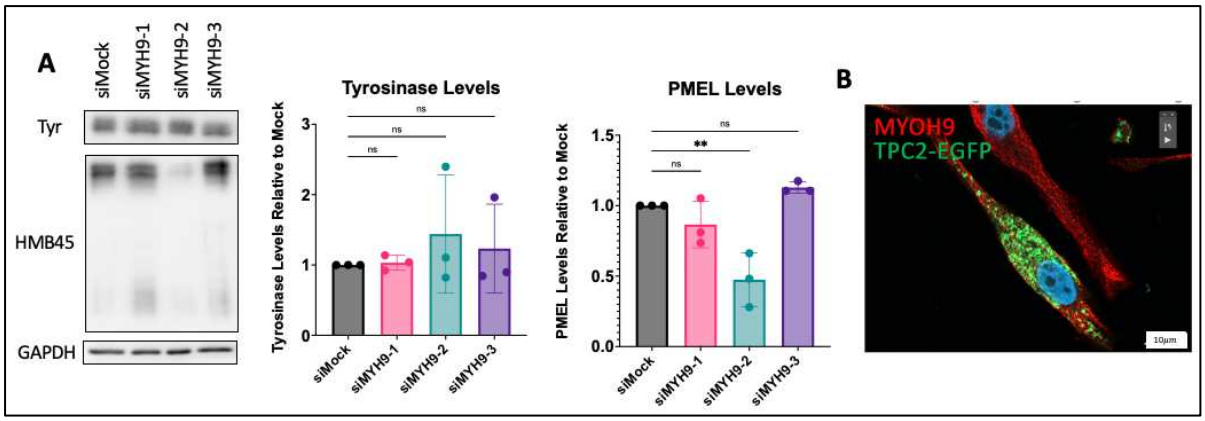

Figure 21: (A) Western blot of tyrosinase (Tyr) and PMEL (HMB45) in total cell extracts from siRNA knockdown cells and corresponding quantification for 3 biological replicates. **(B)** Representative image of confocal fluorescent microscopy for immunostained MYH9 (red) colocalization with exogenously expressed TPC2-EGFP (green) experiment ($10\mu m\ scale\ bar$).

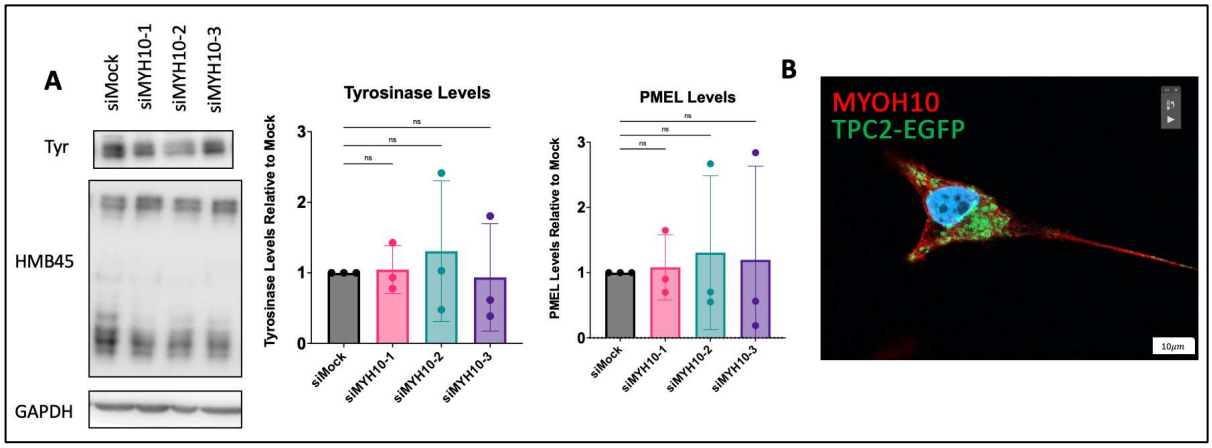

Figure 22: (A) Western blot of tyrosinase (Tyr) and PMEL (HMB45) in total cell extracts from siRNA knockdown cells and corresponding quantification for 3 biological replicates. **(B)** Representative image of confocal fluorescent microscopy for immunostained MYH10 (red) colocalization with exogenously expressed with TPC2-EGFP (green) experiment ($10\mu m$ *scale bar*).

Discussion

Assuming siMYH9-2 was having an off-target effect, the knockdown of both MYH9 and MYH10 gave a hypopigmented phenotype (Table 4). This hypopigmented phenotype supports the hypothesis that MYH9 and MYH10 are functioning in melanosome biogenesis by aiding in the constriction of tubules transporting biogenesis cargo from the endosome to the forming melanosome or in tubules recycling cargo from the melanosome back to the endosome. If the tubules from the endosome to the melanosome are not functioning properly, proteins necessary for proper melanosome biogenesis may not be transported to the melanosome. If the recycling tubules from the melanosome back to the endosome are not functioning properly then biogenesis proteins will not be recycled properly leading to biogenesis defects. While MYH9 and MYH10 are clearly necessary for proper pigmentation, the mechanism behind their involvement needs to be studied further. CRISPR-Cas9 MYH10 knockout cells are currently being developed to confirm the siRNA results and aid in the understanding of MYH10 in melanocytes.

CHAPTER 7: PHOSPHOLIPASE D1 (PLD1)

Background

Phospholipase D (PLD) is a class of transphosphatidylases that hydrolyze phosphatidylcholine (PC) to phosphatidic acid (PA)[57]. PA is a lipid secondary messenger involved in many cellular processes including metabolism, migration, and exocytosis. PLD has been linked to tumor growth and metastasis, neurodegeneration, thrombotic disease, as well as hippocampal axis organization, and proper cardiac development[57–59]. In humans there are two isoforms of PLD, PLD1 and PLD2, with similar structures but very different cellular localization and regulation[57].

Phospholipase D1 (PLD1) localizes to intracellular membranes and upon activation translocates to the plasma membrane[57]. It depends on PI(4,5)P2 as a cofactor and is activated by several protein effectors including GTPases Arf1 and RhoA[57]. Both GTPases, Arf1 and RhoA, are known to be involved in membrane trafficking. PLD1 is most well-known to regulate the formation of lipid droplets in the cytosol, promote dendritic spine development and be a modulator of cancer progression[58,60–62]. Various studies have investigated the role of PLD1 in mouse melanocytes[63,64]; however, a clear understanding of the function of PLD1 in relation to pigment has yet to be discovered.

PLD1 was detected in the TPC2 BioID experiment indicating that it is in the proximity of melanosomes. Based on the previous evidence suggesting PLD1 is involved in melanosome biogenesis, its known localization to intracellular membranes, and its appearance in the TPC2 BioID, PLD1 seemed like a promising candidate in the search for melanosomal membrane proteins. PLD1 is thought to be involved in lipid movement and regulation and, therefore, may

be involved in the formation of many membrane bound organelles, including melanosomes. It may also be localized to melanosome membranes then be activated and translocate to the plasma membrane bringing the whole organelle with it, making it a possible regulator of melanin secretion.

Results

One siRNA was used to generate PLD1 knockdown cells as confirmed by western blotting and immunostaining of PLD1(Figure 23). Both darkness per cell and cell area with pigment showed a hypopigmented phenotype in the PLD1 knockdown cells (Figure 24). The knockdown cells did not show a consistent change in tyrosinase or PMEL levels (Figure 25A), indicating that the phenotype seen is not due to a change in the expression of these enzymes. In preliminary confocal microscopy experiments, immunostained PLD1 appears to colocalize with TPC2-EGFP at melanosome membrane subdomains (Figure 25B).

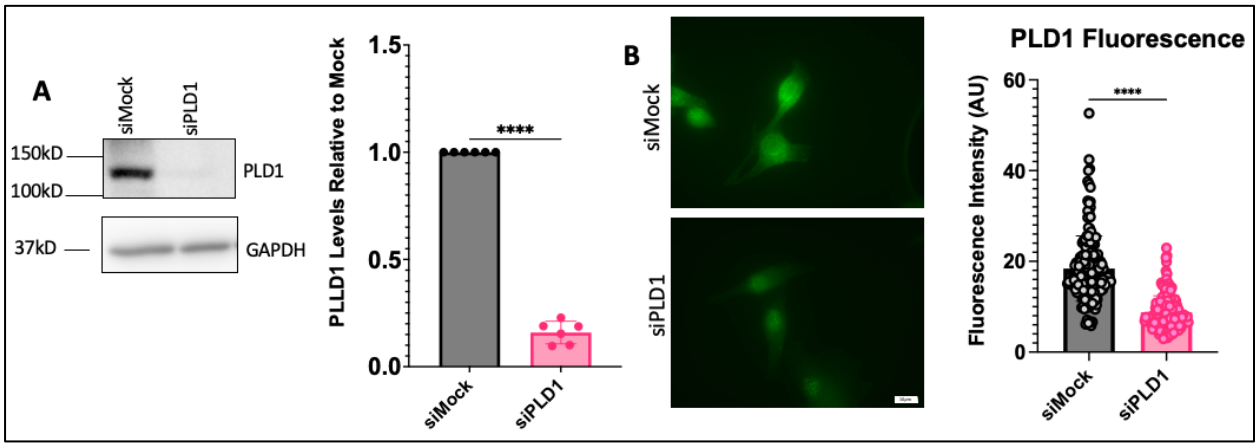

Figure 23: (A) Western blot demonstrating successful knockdown of PLD1 and corresponding quantification for 6 biological replicates. **(B)** Representative widefield fluorescent microscopy images of MNT1 cells transfected with siRNA and immunostained against PLD1 and corresponding fluorescence intensity quantification (siMock n=179 and siPLD1 n=160) ($10\mu m$ *scale bar*).

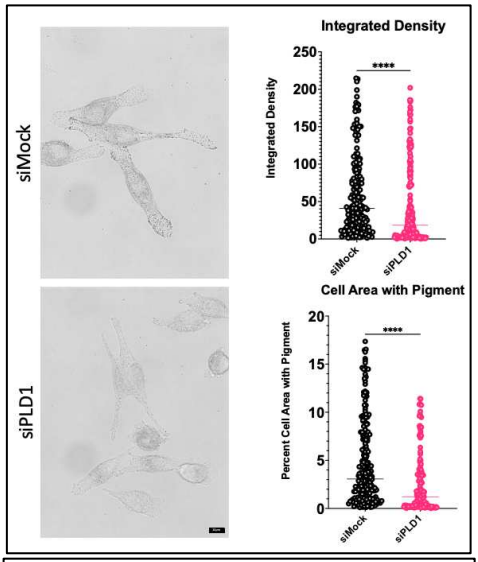

Figure 24: Representative brightfield images and corresponding quantification for integrated density (darkness per cell) and cell area with pigment (siMock n=223 and siPLD1 n=164) ($10\mu m\ scale\ bar$).

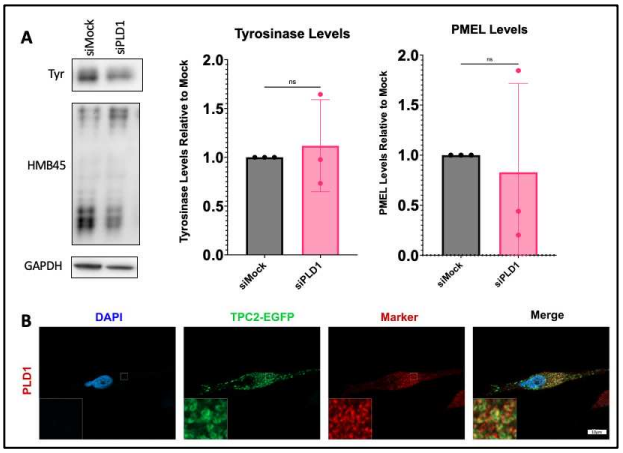

Figure 25: (A) Western blot of tyrosinase (Tyr) and PMEL (HMB45) in total cell extracts from siRNA knockdown cells and corresponding quantification for 3 biological replicates. **(B)** Representative image of confocal fluorescent microscopy for immunostained PLD1 (red) colocalization with exogenously expressed TPC2-EGFP (green) experiment ($10\mu m\ scale\ bar$).

Based on the brightfield and colocalization experiments indicating that PLD1 is involved in regulating overall pigment levels in MNT1 cells and localizes to melanosomes, CRISPR-Cas9 was used to generate PLD1 knockdown MNT1 cells. The success of the knockout was confirmed by western blotting and immunofluorescent staining of PLD1 (Figure 26). The brightfield image analysis was carried out in the PLD1 knockout cells. Knockout cell line 1 (KO1) showed a hypopigmented phenotype but a hyperpigmented phenotype was observed in knockout cell line 2 (KO2) (Figure 27).

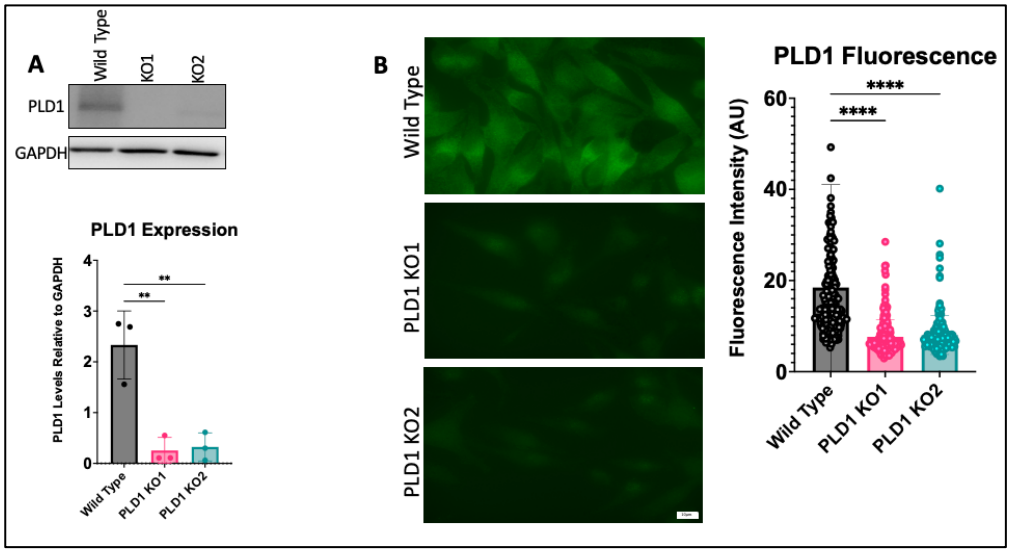

Figure 26: (A) Western blot demonstrating successful knockout of PLD1 and corresponding quantification for 3 biological replicates of the CRISPR-Cas9 knockout cell lysates. **(B)** Representative widefield microscopy images of MNT1 PLD1 knockout cells immunostained against PLD1 and corresponding fluorescence intensity quantification (Wild Type n=232, PLD1 KO1 n=218, and PLD1 KO2 n=198) (10μm *scale bar*).

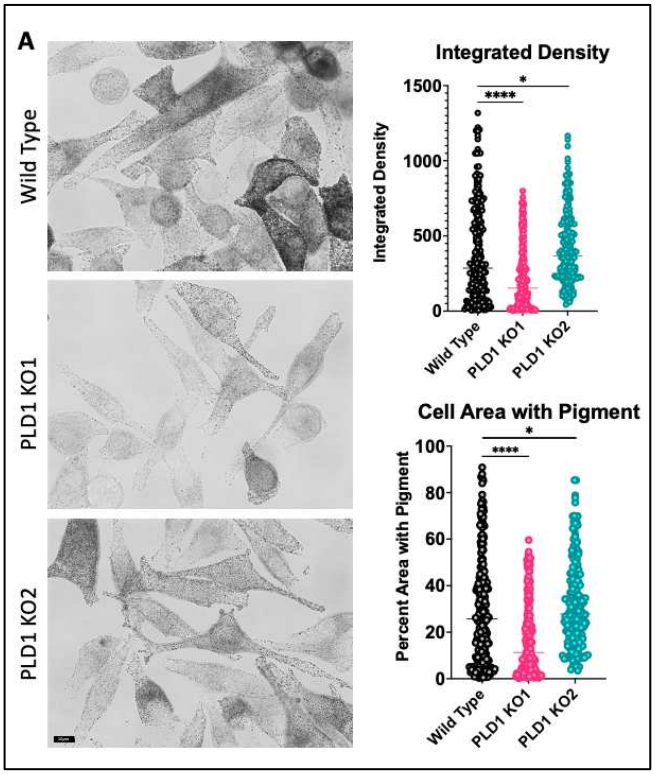

Figure 27: Representative brightfield images and corresponding quantification for integrated density (darkness per cell) and cell area with pigment (Wild Type n=223, PLD1 KO1 n=194, and PLD1 KO2 n=186) (10μm *scale bar*).

Discussion

The inability to consistently confirm the siRNA phenotype in the CRISPR cells as well as the variation in phenotype between the knockout cells suggest that PLD1 may not be directly involved in pigmentation or that the CRISPR had an off-target effect in the cells. Further characterization of the knockout cells, in addition to the production of more knockout cell lines, may help determine if there is a true pigmentation phenotype in cells lacking PLD1.

PLD1 is a key cell signaling molecule involved in many necessary cell processes. It is probable that when PLD1 is not functioning properly in cells, many cell functions such as metabolism, migration, and exocytosis are also not functioning properly. Lack of PLD1 clearly affects pigment levels but it is possibly causing pigmentation changes in an indirect way. PLD1 may be involved in an upstream pathway that eventually regulates pigment, or perhaps the removal of PLD1 from cells overall interferes with the cell's ability to function properly. If PLD1 was directly involved in the pigmentation process a consistent phenotype should be seen when it is knocked down or knocked out of cells. The inability to consistently confirm the siRNA hypopigmentation phenotypes in the two independent CRISPR-Cas9 clones suggests that that the phenotype in one of the clones is due to an off-target effect of the CRISPR and not due to the reduced levels of PLD1.

PLD1 did appear to localize to melanosome membrane subdomains; however, PLD1 is known to be at intracellular membranes rich in PI(4,5)P2 and may localize to multiple intracellular membrane. In the colocalization images there was PLD1 puncta that did not colocalize with TPC2 indicating the PLD1 localization is not specific to melanosome membranes. These results also suggest that PLD1 may be affecting pigmentation in an upstream or indirect way. Since PLD1 appeared to be at melanosomes and give a phenotype, further

experiments are being done to rule out off target effects and characterize the role of PLD1 in MNT1 cells.

CHAPTER 8: MATERIALS AND METHODS

Cell Culture

MNT1 cells were cultured following the previously published protocol[65].

Small Interfering RNA Knockdowns

$1.75X10^6$ MNT1 cells where resuspended in 100µL Lonza SF solution, mixed with 300nM siRNA (Table 2), transferred to Lonza nucleofection cuvette and necleofected using the program DS-137 in a Lonza 4D nucleofector. After 10 minutes, cells were transferred to a 10cm cell culture dish containing 10mL MNT1 media and two 15mm glass coverslips and grown for 72 hours.

Immunofluorescent Staining

After 72 hours of cell growth, coverslips were removed from the 10cm dish and put into a 3cm dish with 2mL Gibco PBS pH 7.4 (1X). After aspirating the PBS, 2mL of 2.5% formaldehyde PBS was added and incubated at 37°C for 15 minutes. The coverslips were washed in 2mL PBS three times and incubated with 2mL blocking buffer (0.1% saponin, 0.05% sodium azide, 1% BSA in PBS) for one hour at room temperature. Coverslips were washed in 2mL PBS three times and incubated with 50µL 1:200 primary antibody in permeabilization buffer (0.1% saponin, 0.05% sodium azide, 0.1% BSA in PBS) for one hour, then washed in 2mL PBS another three times. The coverslips were then incubated for one hour in the dark with 50µL 1:500 AlexaFluor488 or AlexaFluor546 in permeabilization buffer, washed three times with 2mL PBS, and mounted to slides using 10µL Prolong Diamond antifade mountant. Slides were stored in a dark slide holder at 4°C until ready to image.

Brightfield and Widefield Fluorescent Imaging and Analysis

All siRNA knockdown and CRISPR knockout cells were imaged on a BZ-X70 Keyence with a 100X objective lens. All siRNA knockdown cells were imaged and analyzed in a double-blind manner to ensure no bias. All image analysis was done in ImageJ. On brightfield images, cells were circled by hand and then a threshold of 175 was set to pick up pigment. The integrated density measurement was used to determine darkness per cell and the %Area measurement was used to determine the percent cell area with pigment. On fluorescent images, the ROI set from circling cells in brightfield was used to measure the integrated density of the fluorescent images after the background was subtracted to obtain measurements of fluorescence intensity.

Total Cell Lysates

After growing for 72 hours, $1X10^6$ cells were spun down at 200g for 5 minutes then resuspended in 100µL ice cold RIPA Buffer 1X Protease Inhibitor and incubate on ice for 15 minutes, inverting every 5 minutes. Next the samples were centrifuged at 16,000g for 15 minutes and the supernatant was transferred to tubes with 2X sample buffer and stored at -20°C.

Western Blots

Bradford assays were used to determine sample volumes needed to load 40ng of protein on an SDS-Page gel. The SDS-Page gel was ran at 80 volts for 20 minutes and then 120 volts for 90 minutes. The samples were transferred to PVDF membrane at 100 volts, for one hour for all proteins expect the myosins. The myosins were transferred for two hours due to their large size. The PVDF membrane was then block in 5% nonfat milk in TBST for 1 hour at room temperature and incubated with the primary antibody (Table 3) overnight at 4°C. The membrane was washed three times for 5 minutes with TBST and then incubated in secondary HRP antibody for one hour at room temperature then wash in TBST for 5 minutes three times. The membrane was then

imaged using Amersham ECL Prime or Amersham ECL Select (PLD1 only) and analyzed using ImageJ gel analysis. All expression leaves were normalized to the loading control, GAPDH.

Confocal Microscopy

For all candidate proteins except TSPAN10, $3x10^5$ MNT1 cells were transfect with 0.4ng TPC2-EGFP in 20µL Lonza SF solution in a 16 well nucleocuvette strips and nucleofected using program DS-137 in a Lonza 4D nucleofector. The cells were then transferred to 3cm dish containing 15mm coverslips and 2mL of MNT1 media after 10 minutes then grown for 72 hours. Next, they were immunostained against the protein of interest using the protocol describe above with AlexaFluor 546 and imaged on an Airyscan microscope by Wyatt Beyers. For TSPAN10, $3x10^5$ MNT1 cells were transfect with 0.4ng TPC2-iRFP and 0.4ng TSPAN10-EGFP in 20µL Lonza SF solution in a 16 well nucleocuvette strip and nucleofected using program DS-137 in a Lonza 4D nucleofector. After 10 minutes, cells were transferred to 35mm glass bottom dishes with 2mL 37°C KGM Gold media and grown for 24 hours before being imaged. The TPC2-iRFP plasmid was provided by Wyatt Beyers and the TSPAN10-EGFP was cloned out of a plasmid purchased from Horizon Discovery and inserted in the EGFP-C2 vector.

CRISPR-Cas9 Knockouts

MNT1 CRISPR-Cas9 knockouts were generated using the IDT Alt-R CRISPR-Cas9 System. Alt-R CRISPR-Cas9 cRNA and all other CRISPR-Cas9 components were purchased from IDT. Hs.Cas9.TSPAN10.1.AA and Hs.Cas9.TSPAN10.1.AC were used to generate TSPAN10 knockouts. Hs.Cas9.PLD1.1.AA and Hs.Cas9.PLD1.1.AC were used to generate TSPAN10 knockouts.

Rescue and Overexpression Experiments

$3x10^5$ MNT1 cells were transfect with 0.4ng EGFP or TSPAN10-EGFP in 20µL Lonza SF solution in a 16 well nucleocuvette strips and nucleofected using program DS-137 in a Lonza 4D nucleofector. The cells were then transferred to 3cm dish containing 15mm coverslips and 2mL of MNT1 media after 10 minutes then grown for 72 hours. Next, the coverslips were washed, fixed, and mounted. Brightfield and fluorescent imaging was done as described above. To ensure that analysis was done on cells which had the protein of interest reintroduced, only cells which were expressing GFP were analyzed. The TSPAN10-EGFP was cloned out of a plasmid purchased from Horizon Discovery.

Spectrophotometric Melanin Quantification

Melanin Quantification assay in total cell extracts were performed as previously described[11].

Statistical Analysis

GraphPad Prism was used for all graph generation and statistical analysis. Sample distribution normality was determined using the Shapiro-Wilk test. For parametric distributions (western blot analysis and melanin quantification) a Student's T Test was performed and for nonparametric distributions (microscopy analysis) a Mann-Whitney Test was performed. Significance is depicted on graphs as *$P \leq 0.05$; **$P \leq 0.01$; ***$P \leq 0.001$; ****$P \leq 0.0001$ and error bars represent the 95% confidence interval.

REFERENCES

1. Wasmeier, C., Hume, A. N., Bolasco, G. & Seabra, M. C. Melanosomes at a glance. *Journal of Cell Science* **121**, 3995–3999 (2008).
2. Ohbayashi, N. & Fukuda, M. Role of Rab family GTPases and their effectors in melanosomal logistics. *Journal of Biochemistry* vol. 151 343–351 (2012).
3. Chi, A. *et al.* Proteomic and bioinformatic characterization of the biogenesis and function of melanosomes. *Journal of Proteome Research* **5**, 3135–3144 (2006).
4. Graham, M., Tzika, A. C., Mitchell, S. M., Liu, X. & Leonhardt, R. M. Repeat domain-associated O-glycans govern PMEL fibrillar sheet architecture. *Scientific Reports* **9**, (2019).
5. Hurbain, I. *et al. Electron tomography of early melanosomes: Implications for melanogenesis and the generation of fibrillar amyloid sheets*. www.pnas.org/cgi/content/full/ (2008).
6. Hume, A. N. & Seabra, M. C. Melanosomes on the move: a model to understand organelle dynamics. *Biochemical Society transactions* **39**, 1191–1196 (2011).
7. Moreiras, H., Seabra, M. C. & Barral, D. C. Melanin Transfer in the Epidermis: The Pursuit of Skin Pigmentation Control Mechanisms. *International journal of molecular sciences* **22**, (2021).
8. Huizing, M., Helip-Wooley, A., Westbroek, W., Gunay-Aygun, M. & Gahl, W. A. Disorders of lysosome-related organelle biogenesis: clinical and molecular genetics. *Annual review of genomics and human genetics* **9**, 359–386 (2008).

9. Bellono, N. W., Escobar, I. E., Lefkovith, A. J., Marks, M. S. & Oancea, E. An intracellular anion channel critical for pigmentation. *eLife* **3**, e04543 (2014).

10. Fuller, B. B., Spaulding, D. T. & Smith, D. R. Regulation of the catalytic activity of preexisting tyrosinase in black and Caucasian human melanocyte cell cultures. *Experimental cell research* **262**, 197–208 (2001).

11. Ambrosio, A. L., Boyle, J. A., Aradi, A. E., Christian, K. A. & di Pietro, S. M. TPC2 controls pigmentation by regulating melanosome pH and size. *Proceedings of the National Academy of Sciences of the United States of America* **113**, 5622–5627 (2016).

12. Bellono, N. W., Escobar, I. E. & Oancea, E. A melanosomal two-pore sodium channel regulates pigmentation. *Scientific reports* **6**, (2016).

13. Netcharoensirisuk, P. *et al.* Flavonoids increase melanin production and reduce proliferation, migration and invasion of melanoma cells by blocking endolysosomal/melanosomal TPC2. *Scientific reports* **11**, (2021).

14. Sulem, P. *et al.* Two newly identified genetic determinants of pigmentation in Europeans. *Nature genetics* **40**, 835–837 (2008).

15. Roux, K. J., Kim, D. I., Burke, B. & May, D. G. BioID: A Screen for Protein-Protein Interactions. *Current protocols in protein science* **91**, 19.23.1 (2018).

16. Bowman, S. L., Bi-Karchin, J., Le, L. & Marks, M. S. The road to lysosome-related organelles: Insights from Hermansky-Pudlak syndrome and other rare diseases. *Traffic (Copenhagen, Denmark)* **20**, 404–435 (2019).

17. Yamaguchi, Y. & Hearing, V. J. Melanocytes and their diseases. *Cold Spring Harbor perspectives in medicine* **4**, (2014).

18. Matthews, A. L., Szyroka, J., Collier, R., Noy, P. J. & Tomlinson, M. G. Scissor sisters: Regulation of ADAM10 by the TspanC8 tetraspanins. *Biochemical Society Transactions* vol. 45 719–730 (2017).

19. Haining, E. J. *et al.* The TspanC8 subgroup of tetraspanins interacts with a disintegrin and metalloprotease 10 (ADAM10) and regulates its maturation and cell surface expression. *Journal of Biological Chemistry* **287**, 39753–39765 (2012).

20. Harrison, N., Koo, C. Z. & Tomlinson, M. G. Regulation of adam10 by the tspanc8 family of tetraspanins and their therapeutic potential. *International Journal of Molecular Sciences* vol. 22 (2021).

21. Dornier, E. *et al.* Tspanc8 tetraspanins regulate ADAM10/Kuzbanian trafficking and promote Notch activation in flies and mammals. *Journal of Cell Biology* **199**, 481–496 (2012).

22. Kawaguchi, M., Hozumi, Y. & Suzuki, T. ADAM protease inhibitors reduce melanogenesis by regulating PMEL17 processing in human melanocytes. *Journal of Dermatological Science* **78**, 133–142 (2015).

23. van Niel, G. *et al.* The tetraspanin CD63 regulates ESCRT-independent and -dependent endosomal sorting during melanogenesis. *Developmental cell* **21**, 708–721 (2011).

24. Valencia, D. A. & Quinlan, M. E. Formins. *Current biology : CB* **31**, R517–R522 (2021).

25. Kühn, S. & Geyer, M. Formins as effector proteins of rho GTPases. *Small GTPases* **5**, (2014).

26. Bartolini, F. & Gundersen, G. G. Formins and microtubules. *Biochimica et biophysica acta* **1803**, 164–173 (2010).

27. Yang, S. S. *et al.* FMNL2 destabilises COMMD10 to activate NF-κB pathway in invasion and metastasis of colorectal cancer. *British journal of cancer* **117**, 1164–1175 (2017).

28. Gardberg, M., Heuser, V. D., Koskivuo, I., Koivisto, M. & Carpen, O. FMNL2/FMNL3 formins are linked with oncogenic pathways and predict melanoma outcome. *The journal of pathology. Clinical research* **2**, 41–52 (2016).

29. Labat-de-hoz, L. & Alonso, M. A. Formins in human disease. *Cells* **10**, (2021).

30. Kage, F. *et al.* FMNL2 and -3 regulate Golgi architecture and anterograde transport downstream of Cdc42. *Scientific reports* **7**, (2017).

31. Woodham, E. F. *et al.* Coordination by Cdc42 of Actin, Contractility, and Adhesion for Melanoblast Movement in Mouse Skin. *Current biology : CB* **27**, 624–637 (2017).

32. Mendoza-Torreblanca, J. G., Vanoye-Carlo, A., Phillips-Farfán, B. V., Carmona-Aparicio, L. & Gómez-Lira, G. Synaptic vesicle protein 2A: basic facts and role in synaptic function. *The European journal of neuroscience* **38**, 3529–3539 (2013).

33. Bertoglio, D. *et al.* Synaptic vesicle glycoprotein 2A is affected in the CNS of Huntington's Disease mice and post-mortem human HD brain. *Journal of nuclear medicine : official publication, Society of Nuclear Medicine* jnumed.121.262709 (2021) doi:10.2967/JNUMED.121.262709.

34. Menten-Dedoyart, C. *et al.* Development and Validation of a New Mouse Model to Investigate the Role of SV2A in Epilepsy. *PloS one* **11**, (2016).

35. Kong, Y. *et al.* Positron Emission Computed Tomography Imaging of Synaptic Vesicle Glycoprotein 2A in Alzheimer's Disease. *Frontiers in aging neuroscience* **13**, (2021).

36. Löscher, W., Gillard, M., Sands, Z. A., Kaminski, R. M. & Klitgaard, H. Synaptic Vesicle Glycoprotein 2A Ligands in the Treatment of Epilepsy and Beyond. *CNS drugs* **30**, 1055–1077 (2016).

37. Jia, Q. *et al.* Synaptotagmin-4 promotes dendrite extension and melanogenesis in alpaca melanocytes by regulating Ca 2+ influx via TRPM1 channels. *Cell biochemistry and function* **38**, 275–282 (2020).

38. Schnoor, M., Stradal, T. E. & Rottner, K. Cortactin: Cell Functions of A Multifaceted Actin-Binding Protein. *Trends in Cell Biology* **28**, 79–98 (2018).

39. Ammer, A. G. & Weed, S. A. Cortactin branches out: Roles in regulating protrusive actin dynamics. *Cell Motility and the Cytoskeleton* **65**, 687–707 (2008).

40. Jeannot, P. & Besson, A. Cortactin function in invadopodia. *Small GTPases* **11**, 256–270 (2020).

41. Beghein, E., Devriese, D., van Hoey, E. & Gettemans, J. Cortactin and fascin-1 regulate extracellular vesicle release by controlling endosomal trafficking or invadopodia formation and function. *Scientific Reports* **8**, (2018).

42. Ripoll, L. *et al.* Myosin VI and branched actin filaments mediate membrane constriction and fission of melanosomal tubule carriers. *The Journal of cell biology* **217**, 2709–2726 (2018).

43. Althaus, K. & Greinacher, A. MYH9-related platelet disorders. *Seminars in thrombosis and hemostasis* **35**, 189–203 (2009).

44. Pecci, A., Ma, X., Savoia, A. & Adelstein, R. S. MYH9: Structure, functions and role of non-muscle myosin IIA in human disease. *Gene* **664**, 152–167 (2018).

45. Li, T. *et al.* The E3 ligase Ubr3 regulates Usher syndrome and MYH9 disorder proteins in the auditory organs of Drosophila and mammals. *eLife* **5**, (2016).

46. Kim, H. T. *et al.* Myh10 deficiency leads to defective extracellular matrix remodeling and pulmonary disease. *Nature communications* **9**, (2018).

47. Jin, Q. *et al.* Down-regulation of MYH10 driven by chromosome 17p13.1 deletion promotes hepatocellular carcinoma metastasis through activation of the EGFR pathway. *Journal of cellular and molecular medicine* **25**, 11142–11156 (2021).

48. Saultier, P. *et al.* GATA1 pathogenic variants disrupt MYH10 silencing during megakaryopoiesis. *Journal of thrombosis and haemostasis : JTH* **19**, 2287–2301 (2021).

49. Lordier, L. *et al.* RUNX1-induced silencing of non-muscle myosin heavy chain IIB contributes to megakaryocyte polyploidization. *Nature Communications* **3**, (2012).

50. Evans, R. D. *et al.* Myosin-Va and dynamic actin oppose microtubules to drive long-range organelle transport. *Current biology : CB* **24**, 1743–1750 (2014).

51. Jiang, M. *et al.* Microtubule motor transport in the delivery of melanosomes to the actin-rich apical domain of the retinal pigment epithelium. *Journal of cell science* **133**, (2020).

52. Coudrier, E. Myosins in melanocytes: to move or not to move? *Pigment cell research* **20**, 153–160 (2007).

53. Bultema, J. J. *et al.* Myosin vc interacts with Rab32 and Rab38 proteins and works in the biogenesis and secretion of melanosomes. *The Journal of biological chemistry* **289**, 33513–33528 (2014).

54. Gibbs, D. *et al.* Role of myosin VIIa and Rab27a in the motility and localization of RPE melanosomes. *Journal of cell science* **117**, 6473–6483 (2004).

55. Liakath-Ali, K. *et al.* Novel skin phenotypes revealed by a genome-wide mouse reverse genetic screen. *Nature Communications* **5**, (2014).

56. Marini, M. *et al.* Non-muscle myosin heavy chain IIA and IIB interact and co-localize in living cells: Relevance for MYH9-related disease. *International Journal of Molecular Medicine* **17**, 729–736 (2006).

57. Bowling, F. Z., Frohman, M. A. & Airola, M. v. Structure and regulation of human phospholipase D. *Advances in Biological Regulation* vol. 79 (2021).

58. Yao, Y. *et al.* Phospholipase D as a key modulator of cancer progression. *Biological reviews of the Cambridge Philosophical Society* **95**, 911–935 (2020).

59. Riebeling, C., Müller, C. & Geilen, C. C. Expression and regulation of phospholipase D isoenzymes in human melanoma cells and primary melanocytes. *Melanoma research* **13**, 555–562 (2003).

60. Andersson, L. *et al.* PLD1 and ERK2 regulate cytosolic lipid droplet formation. *Journal of cell science* **119**, 2246–2257 (2006).

61. Luo, L. da, Li, G. & Wang, Y. PLD1 promotes dendritic spine development by inhibiting ADAM10-mediated N-cadherin cleavage. *Scientific reports* **7**, (2017).

62. Li, W. Q. *et al.* PLD1 promotes dendritic spine morphogenesis via activating PKD1. *Molecular and cellular neurosciences* **99**, (2019).

63. Ohcuchi, K., Banno, Y., Nakagawa, Y., Akao, Y. & Nozawa, Y. Negative regulation of melanogenesis by phospholipase D1 through mTOR/p70 S6 kinase 1 signaling in mouse B16 melanoma cells. *Journal of cellular physiology* **205**, 444–451 (2005).

64. Ohguchi, K., Banno, Y., Akao, Y. & Nozawa, Y. Involvement of phospholipase D1 in melanogenesis of mouse B16 melanoma cells. *The Journal of biological chemistry* **279**, 3408–3412 (2004).

65. Bultema, J. J., Ambrosio, A. L., Burek, C. L. & di Pietro, S. M. BLOC-2, AP-3, and AP-1 proteins function in concert with Rab38 and Rab32 proteins to mediate protein trafficking to lysosome-related organelles. *Journal of Biological Chemistry* **287**, 19550–19563 (2012).